Journal of Theoretical Biology 580 (2024) 111733

Contents lists available at ScienceDirect

Journal of Theoretical Biology

journal homepage: www.elsevier.com/locate/yjtbi

Stoichiometric microplastics models in natural and laboratory environments

Tianxu Wang, Hao Wang *

Interdisciplinary Lab for Mathematical Ecology & Epidemiology, Department of Mathematical and Statistical Sciences, University of Alberta, Edmonton, Alberta T6G 2G1, Canada

ARTICLE INFO

MSC:
92B05
92D25
34D05
34D23
34C60

Keywords:
Microplastics
Stoichiometric constraints
Light intensity
Nutrients

ABSTRACT

Microplastics pose a severe threat to marine ecosystems; however, relevant mathematical modeling and analysis are lacking. This paper formulates two stoichiometric producer-grazer models to investigate the interactive effects of microplastics, nutrients, and light on population dynamics under different settings. One model incorporates optimal microplastic uptake and foraging behavior based on nutrient availability for natural settings, while the other model does not include foraging in laboratory settings. We establish the well-posedness of the models and examine their long-term behaviors. Our results reveal that in natural environments, producers and grazers exhibit higher sensitivity to microplastics, and the system may demonstrate bistability or tristability. Moreover, the influences of microplastics, nutrients, and light intensity are highly intertwined. The presence of microplastics amplifies the constraints on grazer growth related to food quality and quantity imposed by extreme light intensities, while elevated phosphorus input enhances the system's resistance to intense light conditions. Furthermore, higher environmental microplastic levels do not always imply elevated microplastic body burdens in organisms, as organisms are also influenced by nutrients and light. We also find that grazers are more vulnerable to microplastics, compared to producers. If producers can utilize microplastics for growth, the system displays significantly greater resilience to microplastics.

1. Introduction

Plastic pollution has steadily increased due to widespread plastic use, insufficient disposal practices, and limited waste management capacity over decades. Plastic wastes discharged into terrestrial and aquatic habitats are considered a serious threat to biodiversity, due to their resistance to decomposition (Gall and Thompson, 2015; Carbery et al., 2018). The small plastic particles, ranging from 0.1 μm to 5 mm in size, are called microplastics (EFSA Panel on Contaminants in the Food Chain (CONTAM), 2016). Microplastics are observed almost in all aquatic habitats (Eerkes-Medrano et al., 2015; Peeken et al., 2018). Chronic exposure to microplastics presents several challenges for aquatic organisms (Cui et al., 2017; Duis and Coors, 2016; Nolte et al., 2017; Zhang et al., 2017; Khoironi et al., 2019; Sjollema et al., 2016; Besseling et al., 2014).

Studies have shown that microplastics can be absorbed, concentrated, and transported into various organisms, such as algae. This process significantly hampers algal growth, chlorophyll levels, and photosynthetic activity (Cao et al., 2022; Liu et al., 2019; Chae et al., 2019; Wu et al., 2021; Jiao et al., 2022; Gray and Weinstein, 2017; Zhang et al., 2017; Sjollema et al., 2016; Yang et al., 2020; Ferguson, 2011; Wang et al., 2020; Khoironi et al., 2019; Rodrigues et al., 2019; Salman et al., 2016). This inhibition may occur due to physical factors, such as the blockage of light and airflow (Bhattacharya et al., 2010; Wang et al., 2020; Salman et al., 2016; Bhattacharya et al., 2010), or interactions between microplastics and algae, including adsorption, aggregation (Zhang et al., 2017), and the destruction of algal cell walls through surface absorption (Liu et al., 2019). However, it is worth noting that some laboratory studies suggest that certain algae species may increase in the presence of smaller-sized microplastics, possibly because microplastic particles can be utilized as substrates for the growth of algae (Yokota et al., 2017; Mao et al., 2018; Jiao et al., 2022; Canniff and Hoang, 2018).

Most aquatic animals cannot distinguish plastic from their natural food sources (Sazli et al., 2023). Numerous studies have demonstrated the ingestion of microplastics by a wide range of marine and freshwater species (Lusher, 2015; Scherer et al., 2017), such as cladocerans (Canniff and Hoang, 2018), amphibians (Hu et al., 2016), fish (Lu et al., 2016), and marine mammals (Fossi et al., 2012). These microplastic particles are either selectively ingested, mistaken for prey, or unintentionally consumed during respiration (Gregory, 1996; Derraik, 2002) and may cause long-term accumulation within the digestive tracts. For instance, in filter feeders, microplastics may account for as much as 58% of their stomach content (Goldstein and Goodwin, 2013). Some microplastics are egested but others are internalized and cause a

* Corresponding author.
E-mail address: hao8@ualberta.ca (H. Wang).

https://doi.org/10.1016/j.jtbi.2024.111733
Received 13 September 2023; Received in revised form 27 December 2023; Accepted 8 January 2024
Available online 14 January 2024

series of toxic effects, including reductions in body size, reproduction, food uptake, the onset of oxidative stress and inflammation, and even mortality (Blarer and Burkhardt-Holm, 2016; Alomar et al., 2017; Liu et al., 2019; Wang and Wang, 2023; Guilhermino et al., 2021; Simčič and Anton, 1997; Cui et al., 2017; Canniff and Hoang, 2018; Lin et al., 2023; Elizalde-Velázquez et al., 2020; Martínez-Jerónimo et al., 1994; Bertram and Hart, 1979; Hoffschroeer et al., 2021; Lu et al., 2016; Besseling et al., 2014). For example, Besseling et al. (2014) found that exposure to high-concentration polystyrene particles led to a deformity rate of up to 68% in young daphnia magna. Additionally, Liu et al. (2019) observed that daphnia pulex experienced delayed first clutch timing and a decreased total number of offspring per female at 21 days with the presence of polystyrene microplastics.

Numerous mathematical models have been done to investigate the interaction between environmental toxins and populations by considering the toxic effect on population growth rates (Hallam et al., 1983b,a; De Luna and Hallam, 1987; Freedman and Shukla, 1991; Thomas et al., 1996; Thieme, 2003). Huang et al. (2013) in 2013 proposed a population model incorporating a dose-dependent mortality rate function, and monitored toxin body burdens within a single species. Subsequently, Huang et al. (2015) developed a fundamental model to describe MeHg's effect on predator–prey systems:

$$\begin{aligned}
\frac{dx}{dt} &= \underbrace{r(u,x)x}_{\text{prey growth}} - \underbrace{d_1(u)x}_{\text{prey death}} - \underbrace{f(x)y}_{\text{consumed by predator}},\\
\frac{dy}{dt} &= \underbrace{e(v)f(x)y}_{\text{predator growth from predation}} - \underbrace{d_2(v)y}_{\text{predator death}},\\
\frac{du}{dt} &= \underbrace{\beta_1 T}_{\text{uptake from environment}} - \underbrace{\sigma_1 u}_{\text{depuration}} - \underbrace{r(u,x)u}_{\text{dilution due to growth}},\\
\frac{dv}{dt} &= \underbrace{\beta_2 T}_{\text{uptake from environment}} - \underbrace{\sigma_2 v}_{\text{depuration}} + \underbrace{\xi f(x)u}_{\text{gain due to predation}} - \underbrace{e(v)f(x)v}_{\text{dilution due to growth}}.
\end{aligned} \tag{1.1}$$

Here, x and y (mg C/L) represent prey and predator densities, while u and v (mg M/mg C) represent their respective body toxin burdens. The function $r(u,x)$ characterizes toxin-dependent prey growth, and $d_1(u)$ and $d_2(v)$ are toxicant-related death rates for prey and predator. $f(x)$ and $e(v)$ denote the predator's ingestion rate and toxin-dependent production efficiency, respectively. The parameters a_1 and a_2 represent toxicant uptake rates, and σ_1 and σ_2 are toxin depuration rates for prey and predator. ξ indicates predator toxicant assimilation efficiency.

Notably, none of the aforementioned models considered the influence of food nutrients. However, in natural ecosystems, the growth of species is always constrained by limited nutrient availability (Hecky and Kilham, 1988; Sterner and Hessen, 1994). Organisms require specific proportions of chemical elements, such as carbon (C), nitrogen (N), and phosphorus (P), to meet their fundamental nutritional needs (Ghosh and Chattopadhyay, 2005; Jeyasingh et al., 2017; Ji et al., 2023; Hecky and Kilham, 1988). When these nutritional elements are deficient in the food supply, the conventional predator–prey model may not be applicable since it is the deficiency of nutritional substance, rather than energy content, that constrains the predator growth rate. Instead, stoichiometric models have been widely employed to investigate how nutritional elements influence nutrient cycling mechanisms and population dynamics (Loladze et al., 2000; Li et al., 2011; Xie et al., 2018; Rana et al., 2019; Wang et al., 2012, 2018, 2008; Peace et al., 2013, 2014; Peace, 2015; Chen et al., 2017; Peace and Wang, 2019). Peace and Wang (Peace et al., 2016) in 2016 first expanded upon the basic toxin population model to explore the interactive influence of nutrients and MeHg on population dynamics by incorporating stoichiometric constants into growth rates of producers and grazers.

In laboratory experiments, the conditions for organisms are manually controlled. Typically, grazers are provided with food directly in a small confined container and almost do not need to forage. However, in natural environments, grazers must expend significant energy and time on foraging and deal with challenges like predation risk, extreme climates, and human interactions. Their foraging strategies have been shown to depend on the nutritional content of their food (Simpson et al., 2004; Schatz and McCauley, 2007). When food is nutrient-deficient, grazers have to allocate more time to eat more food to meet their nutrient requirements (Raubenheimer and Simpson, 1993).

Although microplastics have been shown to highly threaten aquatic ecosystems and have garnered increasing concern in recent years, there is currently no mathematical model to investigate their influence on population dynamics. Considering the differences between laboratory settings and natural ecosystems, this paper aims to develop two stoichiometric models to explore how microplastics influence producer-grazer population dynamics in different settings: one model includes optimal microplastic uptake and foraging behavior based on nutrient availability for natural settings, while the other model does not consider foraging behavior for laboratory settings.

2. Model formulation

This study focuses on the interaction between producers (e.g., algae) and grazers (e.g., Daphnia) in a closed ecosystem. The overall framework is based on the general toxin model (1.1). First, we decide the growth rate function. Similar to Huang et al. (2015), we assume the influence of microplastics on the growth of producers and grazers follows a linear response:

$$\max\{0, 1-\alpha_2 u\} \tag{2.1}$$

and

$$\max\{0, 1-\beta_2 v\}, \tag{2.2}$$

where α_2 and β_2 are the influence coefficients of microplastics on the producer growth and gazer reproduction, respectively.

Meanwhile, the growth of producers and predators is also influenced by their internal nutrient element reserves, such as carbon (C) and phosphorus (P). The stoichiometric limitations have a substantial impact on trophic transfer efficiencies (Peace, 2015). We adhere to the classic assumption of a closed phosphorus system, where the P:C ratio varies in producers and remains constant in grazers (Loladze et al., 2000). The total phosphorus content is denoted as P. We introduce a variable P:C ratio denoted as Q for producers, with a minimum value of q, and a constant P:C ratio represented by θ for grazers. Then Q is given by

$$Q = \frac{P-\theta y}{x}. \tag{2.3}$$

Moreover, light intensity plays a crucial role in producers' photosynthesis and growth. Therefore, the growth rate of producers and grazers, influenced by light and nutrients, can be represented by:

$$\alpha_1 \min\left\{1-\frac{x}{K}, 1-\frac{q}{Q}\right\} \tag{2.4}$$

and

$$\beta_1 \min\left\{1, \frac{Q}{\theta}\right\}. \tag{2.5}$$

Here, α_1 and β_1 denote the maximal growth rate and production rate of the producer and grazer, respectively. K represents the maximal producer carrying capacity with respect to light.

Incorporating (2.1), (2.2), (2.4) and (2.5), the growth rate function of producers and the production efficiency function of grazers can be modeled using following minimum functions:

$$r(u,x) = \alpha_1 \min\left\{\max\{0, 1-\alpha_2 u\}, 1-\frac{x}{K}, 1-\frac{q}{Q}\right\},$$

$$e(v) = \beta_1 \min\left\{\max\{0, 1-\beta_2 v\}, \frac{Q}{\theta}\right\}.$$

Table 2.1
Parameter values. Further elaboration in Appendix.

Para.	Description	Value	Unit	Reference
α_1	Maximal growth rate of producer	1.2	1/day	Andersen (2013)
α_2	microplastic impact on producer growth	0.05(−0.0989–1.9)	mg C/mg M	Yang et al. (2020), Zhang et al. (2017)
β_1	Maximal production efficiency of grazer	0.8	no unit	Andersen (2013)
β_2	Microplastic impact on grazer reproduction	10(8.7–15.78)	mg C/mg M	Guilhermino et al. (2021)
h_2	Microplastic impact on grazer mortality	0.2(0.11–0.29)	mg C/mg M/day	Guilhermino et al. (2021)
m_2	Grazer natural death rate	0.025(0.0206–0.25)	1/day	Bertram and Hart (1979), Andersen (2013)
a_1	Producer microplastic uptake rate (adsorption and absorption capacity)	0.006(0.0056–0.0131)	L/mg C/day	Bhattacharya et al. (2010)
a_2	Food nutrient impact on producer microplastic uptake	0.001	L/mg C/day	
b_1	Grazer microplastic uptake rate	0.0009(0.00073–0.00096)	L/mg C/day	Elizalde-Velázquez et al. (2020)
σ_1	Decomposition rate for producer	0.0051	1/day	Canniff and Hoang (2018)
σ_2	Depuration rate for grazer	0.08(0.0712–0.25)	1/day	Elizalde-Velázquez et al. (2020)
a	Grazer ingestion half saturation constant	0.0012–0.25	mg C/L/day	Peace and Wang (2019), Andersen (2013)
c	Maximal ingestion rate of grazer	0.81	1/day	Andersen (2013)
$\eta(Q)$	Feeding effort function	$\eta_1 = 5.17, \eta_2 = -0.31, \eta_3 = 0.007$		Peace and Wang (2019)
q	Algae minimal P:C ratio	0.0038	mg P/mg C	Andersen (2013)
$\hat{Q}$	algae maximal P:C ratio	2.5	mg P/mg C	Peace and Wang (2019)
θ	Daphnia P:C ratio	0.03	mg P/mg C	Andersen (2013)
ξ	Daphnia microplastic assimilation efficiency	0.97	no unit	
T	Total toxin concentration in environment	0–3	mg M/L	
K	Producer maximal carrying capacity	0–5	mg C/L	
P	Total phosphorus	0–0.05	mg C/L	

We assume that the death rate of grazers is linearly proportional to their microplastic body burden (Huang et al., 2015) and the death rate function is given by

$$d_2(v) = h_2 v + m_2,$$

where m_2 is the natural death rate, h_2 is a influence coefficient.

For the natural ecosystem, grazers exhibit robust foraging capability in response to spatial variations in food quality. For example, Daphnia has been observed selectively foraging in regions of higher food quality, even though comparable carbon ingestion rates could be achieved elsewhere (Schatz and McCauley, 2007). Hence, we consider the predation functional response with optimal foraging as:

$$f(x,Q) = \frac{c\eta(Q)x}{a + \eta(Q)x}, \tag{2.6}$$

where the feeding effort is given by Peace and Wang (2019)

$$\eta(Q) = \eta_1 Q^2 + \eta_2 Q + \eta_3. \tag{2.7}$$

The parameter c represents the maximal production efficiency, and a is the half-saturation constant.

Apart from the concentration of environmental microplastics, the response of producers and grazers to microplastics is strongly influenced by internal nutrient levels. When their nutrient levels are low, they must enhance resource absorption from the environment, unavoidably resulting in increased microplastic uptake. On the other hand, plankton absorbs microplastics through phospholipids. With less phosphorus, phospholipids in plankton are actually more abundant (Gašparovic et al., 2023), thereby increasing microplastic uptake. Therefore, we consider the microplastic uptake rate to be a decreasing function of the internal nutrient level. The microplastic uptake function for producers takes the following form:

$$L_1(Q) = a_1 + a_2 \frac{\hat{Q} - Q}{Q - q}. \tag{2.8}$$

Here, a_1 and a_2 are the uptake rates of microplastic particles for producers. Since the nutrient level in grazers is assumed to be constant, the microplastic uptake function for grazers is also constant:

$$L_2(\theta) = b_1. \tag{2.9}$$

We now introduce our stoichiometric model incorporating optimal microplastic uptake and foraging (OMUF model) under a natural environment as follows:

$$\begin{aligned}
\frac{dx}{dt} &= \underbrace{\alpha_1 \min\left\{\max\{0, 1-\alpha_2 u\}, 1-\frac{x}{K}, 1-\frac{q}{Q}\right\} x}_{\text{producer growth}} - \underbrace{f(x,Q)y}_{\text{consumed by grazer}}, \\
\frac{dy}{dt} &= \underbrace{\beta_1 \min\left\{\max\{0, 1-\beta_2 v\}, \frac{Q}{\theta}\right\} f(x,Q)y}_{\text{grazer growth from predation}} \\
&\quad - \underbrace{\eta(Q)y}_{\text{cost of feeding effort}} - \underbrace{(h_2 v + m_2)y}_{\text{grazer death}}, \\
\frac{du}{dt} &= \underbrace{L_1(Q)T}_{\text{uptake from environment}} - \underbrace{\sigma_1 u}_{\text{decomposition}} \\
&\quad - \underbrace{\alpha_1 \min\left\{\max\{0, 1-\alpha_2 u\}, 1-\frac{x}{K}, 1-\frac{q}{Q}\right\} u}_{\text{dilution due to growth}}, \\
\frac{dv}{dt} &= \underbrace{L_2(\theta)T}_{\text{uptake from environment}} - \underbrace{\sigma_2 v}_{\text{depuration}} + \underbrace{\xi f(x,Q)u}_{\text{gain due to predation}} \\
&\quad - \underbrace{\beta_1 \min\left\{\max\{0, 1-\beta_2 v\}, \frac{Q}{\theta}\right\} f(x,Q)v}_{\text{dilution due to growth}},
\end{aligned} \tag{2.10}$$

where Q, $f(x,Q)$, $\eta(Q)$, $L_1(Q)$, and $L_2(\theta)$ are defined in (2.3), (2.6), (2.7), (2.8), and (2.9), respectively.

In the laboratory setting, the foraging cost for grazers is negligible. For simplicity, the uptake rate of microplastics by producers is assumed to be constant. This leads to the non-foraging microplastics model (NM model):

$$\begin{aligned}
\frac{dx}{dt} &= \underbrace{\alpha_1 \min\left\{\max\{0, 1-\alpha_2 u\}, 1-\frac{x}{K}, 1-\frac{q}{Q}\right\} x}_{\text{producer growth}} - \underbrace{f(x)y}_{\text{consumed by grazer}}, \\
\frac{dy}{dt} &= \underbrace{\beta_1 \min\left\{\max\{0, 1-\beta_2 v\}, \frac{Q}{\theta}\right\} f(x)y}_{\text{grazer growth from predation}} - \underbrace{(h_2 v + m_2)y}_{\text{grazer death}},
\end{aligned}$$

$$\begin{aligned}\frac{\mathrm{d}u}{\mathrm{d}t} =& \underbrace{a_1 T}_{\text{uptake from environment}} - \underbrace{\sigma_1 u}_{\text{decomposition}} \\ &\underbrace{- \alpha_1 \min\left\{\max\{0, 1-\alpha_2 u\}, 1-\frac{x}{K}, 1-\frac{q}{Q}\right\} u}_{\text{dilution due to growth}}, \\ \frac{\mathrm{d}v}{\mathrm{d}t} =& \underbrace{b_1 T}_{\text{uptake from environment}} - \underbrace{\sigma_2 v}_{\text{depuration}} + \underbrace{\xi f(x) u}_{\text{gain due to predation}} \\ &\underbrace{- \beta_1 \min\left\{\max\{0, 1-\beta_2 v\}, \frac{Q}{\theta}\right\} f(x) v}_{\text{dilution due to growth}},\end{aligned} \tag{2.11}$$

where

$$f(x) = \frac{cx}{a+x}.$$

3. Mathematical analysis

Separate mathematical analyses are conducted for the two models. let us begin with the OMUF model.

3.1. The OMUF model

The body burden dynamics are assumed to operate on a much faster timescale than population dynamics. Over a long period, the body burden accumulation will reach an equilibrium, allowing the body burden dynamics to attain a quasi-steady state. To simplify the model, we introduce a small parameter, $\epsilon = \alpha_1\sigma_1$, for rescaling the model. In our case, $\epsilon = 0.0061$. We then apply the quasi-steady state approximation to reduce our model to a two-dimensional form. The well-posedness and long-term behavior of the resulting two-dimensional systems are then explored.

3.1.1. Rescaling and quasi-steady-state approximation

Rescale the model (2.10) as follows:

$\tilde{u} = \alpha_2 u$, $\widetilde{m_2} = \frac{m_2}{\alpha_1}$, $\tilde{\eta_1} = \frac{\eta_1}{\alpha_1}$, $\tilde{\eta_2} = \frac{\eta_2}{\alpha_1}$, $\tilde{\eta_3} = \frac{\eta_3}{\alpha_1}$, $\widetilde{\beta_1} = \frac{c\beta_1}{\alpha_1}$, $\widetilde{\beta_2} = \frac{\xi c\sigma_1\beta_2}{\alpha_2}$, $\tilde{v} = \beta_2 v$, $\epsilon = \alpha_1\sigma_1$, $\tilde{t} = \alpha_1 t$, $\widetilde{\sigma_2} = \sigma_2\sigma_1$, $\tilde{y} = \frac{c}{\alpha_1}y$, $\widetilde{h_2} = \frac{h2}{\beta_2\alpha_1}$, $\tilde{\theta} = \frac{\alpha_1\theta}{c}$, $\tilde{Q} = \frac{P-\tilde{\theta}\tilde{y}}{x}$, $\tilde{a_1} = a_1\alpha_2\sigma_1$, $\tilde{a_2} = a_2\alpha_2\sigma_1$, $\tilde{b_1} = b_1\beta_2\sigma_1$, $\widetilde{L_1} = \tilde{a_1} + \tilde{a_2}\frac{\hat{Q}-\tilde{Q}}{\hat{Q}-q}$, $\widetilde{L_2} = \tilde{b_1}$.

For simplicity, we still use the original notation instead of the tilde notation. The rescaled model is given as follows:

$$\begin{aligned}\frac{\mathrm{d}x}{\mathrm{d}t} &= \alpha_1 \min\left\{\max\{0, 1-u\}, 1-\frac{x}{K}, 1-\frac{q}{Q}\right\} x - \frac{\eta(Q)xy}{a+\eta(Q)x}, \\ \frac{\mathrm{d}y}{\mathrm{d}t} &= \beta_1 \min\left\{\max\{0, 1-v\}, \frac{Q}{\theta}\right\} \frac{\eta(Q)xy}{a+\eta(Q)x} - \eta(Q)y - (h_2 v + m_2)y, \\ \epsilon\frac{\mathrm{d}u}{\mathrm{d}t} &= L_1(Q)T - \sigma_1^2 u - \epsilon \min\left\{\max\{0, 1-u\}, 1-\frac{x}{K}, 1-\frac{q}{Q}\right\} u, \\ \epsilon\frac{\mathrm{d}v}{\mathrm{d}t} &= L_2(\theta)T - \sigma_2 v + \beta_2\frac{\eta(Q)x}{a+\eta(Q)x}u - \epsilon\beta_1 \min\left\{\max\{0, 1-v\}, \frac{Q}{\theta}\right\} \frac{\eta(Q)x}{a+\eta(Q)x} v.\end{aligned} \tag{3.1}$$

Let $\epsilon \to 0$, the system (3.1) reaches a quasi-steady system with

$$u = \frac{L_1(Q)T}{\sigma_1^2}, \quad v = \frac{L_2(\theta)T}{\sigma_2} + \frac{\beta_2 L_1(Q)T}{\sigma_2\sigma_1^2}\frac{\eta(Q)x}{a+\eta(Q)x}. \tag{3.2}$$

Let

$$A_1 = 1 - \frac{L_2(\theta)T}{\sigma_2}, \tag{3.3}$$

$$A_2 = \frac{\beta_2 T}{\sigma_2\sigma_1^2} > 0. \tag{3.4}$$

Substituting (3.2) into (3.1), we have

$$\begin{aligned}\frac{\mathrm{d}x}{\mathrm{d}t} =& \alpha_1 \min\left\{\max\left\{0, 1-\frac{L_1(Q)T}{\sigma_1^2}\right\}, 1-\frac{x}{K}, 1-\frac{q}{Q}\right\} x - \frac{\eta(Q)xy}{a+\eta(Q)x}, \\ \frac{\mathrm{d}y}{\mathrm{d}t} =& \beta_1 \min\left\{\max\left\{0, A_1 - A_2 L_1(Q)\frac{\eta(Q)x}{a+\eta(Q)x}\right\}, \frac{Q}{\theta}\right\} \frac{\eta(Q)xy}{a+\eta(Q)x} \\ &- \eta(Q)y - \left(h_2\left(1 - A_1 + A_2 L_1(Q)\frac{\eta(Q)x}{a+\eta(Q)x}\right) + m_2\right) y.\end{aligned} \tag{3.5}$$

3.1.2. Positivity and boundedness

Let

$$\Omega = \left\{(x, y) : 0 \le x \le k, y \ge 0, qx + \theta y < P\right\}, \tag{3.6}$$

where $k = \min\left\{\frac{P}{q}, K\right\}$. The following theorem guarantees that system (3.5) is biologically well defined.

Theorem 3.1. *Solutions of (3.5) with initial conditions in the Ω remain there for all forward time.*

Proof. Assume $S(t) = (x(t), y(t))$ is a solution of system (3.5) with $S(0) \in \Omega$ and t_1 is the first time that $S(t)$ touches or crosses the boundary of Ω. We will prove the theorem by contradiction arguments from five cases.

Case 1. $x(t_1) = 0$. Let $\hat{y} = \max_{t\in[0,t_1]} y(t) < \frac{P}{\theta}$, $\hat{\eta} = \max_{t\in[0,t_1]}\eta(Q(t))$. Then $\forall t \in [0, t_1]$,

$$\begin{aligned}\frac{\mathrm{d}x}{\mathrm{d}t} &= \alpha_1 \min\left\{\max\left\{0, 1-\frac{L_1(Q)T}{\sigma_1^2}\right\}, 1-\frac{x}{K}, 1-\frac{q}{Q}\right\} x - \frac{\eta(Q)xy}{a+\eta(Q)x} \\ &\ge -\frac{\eta(Q)xy}{a+\eta(Q)x} \\ &\ge -\frac{\hat{\eta}\hat{y}}{a}x \equiv \delta_1 x,\end{aligned}$$

where δ_1 is a constant. Thus, $x(t_1) \ge x(0)e^{\delta_1 t_1} > 0$ holds, which contradicts with $x(t_1) = 0$. Therefore, $S(t_1)$ cannot reach this boundary.

Case 2. $y(t_1) = 0$. Let $\hat{x} = \max_{t\in[0,t_1]} x(t) \le k = \min\left\{K, \frac{P}{q}\right\}$. $\forall t \in [0, t_1]$,

$$\begin{aligned}\frac{\mathrm{d}y}{\mathrm{d}t} &\ge -\eta(Q)y - \left(h_2\left(1 - A_1 + A_2 L_1(Q)\frac{\eta(Q)x}{a+\eta(Q)x}\right) + m_2\right) y \\ &\ge -\left(\hat{\eta} + h_2\left(1 - A_1 + A_2(a_1+a_2)\frac{\hat{\eta}\hat{x}}{a}\right) + m_2\right) y \equiv \delta_2 y,\end{aligned}$$

where δ_2 is a constant. Thus, $y(t_1) \ge y(0)e^{\delta_2 t_1} > 0$ holds, which contradicts with $y(t_1) = 0$. Therefore, $S(t_1)$ cannot reach this boundary.

Case 3. $x(t_1) = k$.

$$\left.\frac{\mathrm{d}x}{\mathrm{d}t}\right|_{t=t_1} = \alpha_1 \min\left\{\max\left\{0, 1-\frac{L_1(Q)T}{\sigma_1^2}\right\}, 1-\frac{x}{K}, 1-\frac{q}{Q}\right\} x - \frac{\eta(Q)xy}{a+\eta(Q)x} \le 0.$$

Therefore, $S(t_1)$ cannot cross this boundary.

Case 4. $qx(t_1) + \theta y(t_1) = P$, i.e., $Q(t_1) = q$. It follows that

$$\alpha_1 \min\left\{\max\left\{0, 1-\frac{L_1(Q)T}{\sigma_1^2}\right\}, 1-\frac{x}{K}, 1-\frac{q}{Q}\right\} x\Big|_{t=t_1} = 0.$$

Since $\beta_1 < 1$,

$$\begin{aligned}&\left.\frac{\mathrm{d}(qx+\theta y)}{\mathrm{d}t}\right|_{t=t_1} \\ =& q\frac{\mathrm{d}x(t_1)}{\mathrm{d}t} + \theta\frac{\mathrm{d}y(t_1)}{\mathrm{d}t} \\ \le& -\frac{q\eta(Q)xy}{a+\eta(Q)x} + \theta\beta_1 \min\left\{\max\left\{0, A_1 - A_2 L_1(Q)\frac{\eta(Q)x}{a+\eta(Q)x}\right\}, \frac{Q}{\theta}\right\} \frac{\eta(Q)xy}{a+\eta(Q)x} \\ \le& -\frac{q\eta(Q)xy}{a+\eta(Q)x} + \frac{\beta_1 q\eta(Q)xy}{a+\eta(Q)x} < 0.\end{aligned}$$

This implies that $S(t_1)$ cannot cross this boundary.

In summary, the solution $S(t)$ of system (3.5) starting from Ω will stay in Ω for all forward time. This completes the proof. □

3.1.3. Equilibrium analysis

In this section, we analyze the stability of equilibria to investigate the long-term behavior of the system. To simplify the analysis, we rewrite (3.5) as follows:

$$\frac{dx}{dt} = xF_1(x,y),$$
$$\frac{dy}{dt} = yG_1(x,y),$$

where

$$F_1(x,y) = \alpha_1 \min\left\{\max\left\{0, 1-\frac{L_1(Q)T}{\sigma_1^2}\right\}, 1-\frac{x}{K}, 1-\frac{q}{Q}\right\} - \frac{\eta(Q)y}{a+\eta(Q)x},$$
$$G_1(x,y) = \beta_1 \min\left\{\max\left\{0, A_1 - A_2L_1(Q)\frac{\eta(Q)x}{a+\eta(Q)x}\right\}, \frac{Q}{\theta}\right\}\frac{\eta(Q)x}{a+\eta(Q)x} - \eta(Q) - \left(h_2\left(1-A_1+A_2L_1(Q)\frac{\eta(Q)x}{a+\eta(Q)x}\right)+m_2\right).$$

For the local stability of equilibria, we apply the method of the Jacobian matrix (Loladze et al., 2000), where

$$J(x,y) = \begin{pmatrix} F_1 + xF_{1_x}(x,y) & xF_{1_y}(x,y) \\ yG_{1_x}(x,y) & G_1 + yG_{1_y}(x,y)\end{pmatrix}.$$

Theorem 3.2. *The extinction equilibrium $E_0(0,0)$ is unstable.*

Proof. At $E_0(0,0)$, the Jacobian matrix is given by

$$J(E_0) = \begin{pmatrix} F_1(0,0) & 0 \\ 0 & -\left(\frac{h_2b_1T}{\sigma_2}+m_2\right)\end{pmatrix},$$

where $F_1(0,0) = \begin{cases} \alpha_1 \max\left\{0, 1-\frac{a_1T}{\sigma_1^2}\right\} \geq 0, & a_2 = 0, \\ \alpha_1 > 0, & a_2 \neq 0. \end{cases}$

Since the eigenvalues have different signs, E_0 is unstable. □

Biologically, this implies that this ecosystem will never collapse completely.

Theorem 3.3. *The producer-only equilibrium $E_1(k,0)$ is locally asymptotically stable (LAS) if $G_1(k,0) < 0$; otherwise, it is unstable.*

Proof. At $E_1(k,0)$, the Jacobian matrix is given by

$$J(E_1) = \begin{pmatrix} kF_{1_x}(k,0) & kF_{1_y}(k,0) \\ 0 & G_1(k,0)\end{pmatrix}.$$

It is easy to calculate that $kF_{1_x}(k,0) < 0$, therefore, if $G_1(k,0) > 0$, then E_1 is unstable; otherwise, E_1 is LAS. □

This indicates that when the growth rate of grazers is less than their death rate, grazers will die out and producers will stabilize at $k = \min\{K, P/q\}$ eventually.

3.2. The NM model

Through similar rescaling and letting $\epsilon \to 0$, we obtain a quasi-steady system with

$$u = \frac{a_1T}{\sigma_1^2}, \quad v = \frac{T}{\sigma_2}\left(b_1 + \frac{a_1\beta_2}{\sigma_1^2}\frac{x}{a+x}\right). \tag{3.7}$$

Let $B_1 = \max\left\{0, 1-\frac{a_1T}{\sigma_1^2}\right\}$, $B_2 = A_2a_1$, where A_2 is given by (3.4). The degenerated two-dimensional equation is then given by

$$\frac{dx}{dt} = \alpha_1 \min\left\{B_1, 1-\frac{x}{K}, 1-\frac{q}{Q}\right\}x - \frac{xy}{a+x},$$
$$\frac{dy}{dt} = \beta_1 \min\left\{\max\left\{0, A_1 - B_2\frac{x}{a+x}\right\}, \frac{Q}{\theta}\right\}\frac{x}{a+x}y - \left(h_2\left(1-A_1+B_2\frac{x}{a+x}\right)+m_2\right)y. \tag{3.8}$$

Using a similar argument, it can be shown that Ω remains the invariant set of (3.8), and the stability analysis of boundary equilibria for the system (3.8) can also be determined by Theorems 3.2 and 3.3. Detailed proofs will not be provided here. We now proceed to determine the stability of internal equilibria.

Rewrite (3.8) as

$$\frac{dx}{dt} = xF_2(x,y),$$
$$\frac{dy}{dt} = yG_2(x,y).$$

Here,

$$F_2(x,y) = \alpha_1 \min\left\{B_1, 1-\frac{x}{K}, 1-\frac{q}{Q}\right\} - \frac{y}{a+x} = \begin{cases} \alpha_1B_1 - \frac{y}{a+x}, \\ \quad x \leq K(1-B_1), qx+\theta(1-B_1)y \leq (1-B_1)P, \\ \alpha_1\left(1-\frac{x}{K}\right) - \frac{y}{a+x}, \\ \quad x > K(1-B_1), y \leq \frac{P-qK}{\theta}, \\ \alpha_1\left(1-\frac{qx}{P-\theta y}\right) - \frac{y}{a+x}, \\ \quad qx+\theta(1-B_1)y > (1-B_1)P, y > \frac{P-qK}{\theta}. \end{cases}$$

If $A_1 < B_2$,

$$G_2(x,y) = \begin{cases} -\left(h_2\left(1-A_1+B_2\frac{x}{a+x}\right)+m_2\right), \\ \quad x > \frac{aA_1}{B_2-A_1}, \\ \beta_1\left(A_1-B_2\frac{x}{a+x}\right)\frac{x}{a+x} - \left(h_2\left(1-A_1+B_2\frac{x}{a+x}\right)+m_2\right), \\ \quad x \leq \frac{aA_1}{B_2-A_1}, \left(A_1-B_2\frac{x}{a+x}\right)x + y \leq \frac{P}{\theta}, \\ \beta_1\frac{P-\theta y}{\theta x}\frac{x}{a+x} - \left(h_2\left(1-A_1+B_2\frac{x}{a+x}\right)+m_2\right), \\ \quad x \leq \frac{aA_1}{B_2-A_1}, \left(A_1-B_2\frac{x}{a+x}\right)x + y > \frac{P}{\theta}. \end{cases}$$

If $A_1 \geq B_2$,

$$G_2(x,y) = \begin{cases} \beta_1\left(A_1-B_2\frac{x}{a+x}\right)\frac{x}{a+x} - \left(h_2\left(1-A_1+B_2\frac{x}{a+x}\right)+m_2\right), \\ \quad \left(A_1-B_2\frac{x}{a+x}\right)x + y \leq \frac{P}{\theta}, \\ \beta_1\frac{P-\theta y}{\theta x}\frac{x}{a+x} - \left(h_2\left(1-A_1+B_2\frac{x}{a+x}\right)+m_2\right), \\ \quad \left(A_1-B_2\frac{x}{a+x}\right)x + y > \frac{P}{\theta}. \end{cases}$$

The derivatives of $F_2(x,y)$ and $G_2(x,y)$ are given as follows:

$$F_{2_x} = \begin{cases} \frac{y}{(a+x)^2} > 0, & x < K(1-B_1), qx+\theta(1-B_1)y < (1-B_1)P, \\ -\frac{\alpha_1}{K} + \frac{y}{(a+x)^2}, & x > K(1-B_1), y < \frac{P-qK}{\theta}, \\ -\frac{\alpha_1 q}{P-\theta y} + \frac{y}{(a+x)^2}, & qx+\theta(1-B_1)y > (1-B_1)P, y > \frac{P-qK}{\theta}. \end{cases}$$

$$F_{2_y} = \begin{cases} -\frac{1}{a+x} < 0, & x < K(1-B_1), qx+\theta(1-B_1)y < (1-B_1)P, \\ -\frac{1}{a+x} < 0, & x > K(1-B_1), y < \frac{P-qK}{\theta}, \\ -\frac{\alpha_1\theta q}{(P-\theta y)^2} - \frac{1}{a+x} < 0, & qx+\theta(1-B_1)y > (1-B_1)P, y > \frac{P-qK}{\theta}. \end{cases}$$

If $A_1 < B_2$, we have

$$G_{2_x} = \begin{cases} -h_2B_2\frac{a}{(a+x)^2} < 0, \\ \quad x > \frac{aA_1}{B_2-A_1}, \\ -\beta_1B_2\frac{2ax}{(a+x)^3} + (\beta_1A_1 - h_2B_2)\frac{a}{(a+x)^2}, \\ \quad x < \frac{aA_1}{B_2-A_1}, \left(A_1-B_2\frac{x}{a+x}\right)x + y < \frac{P}{\theta}, \\ -\frac{\beta_1}{\theta}\frac{P-\theta y}{(a+x)^2} - h_2B_2\frac{a}{(a+x)^2} < 0, \\ \quad x < \frac{aA_1}{B_2-A_1}, \left(A_1-B_2\frac{x}{a+x}\right)x + y > \frac{P}{\theta}. \end{cases}$$

$$G_{2_y}=\begin{cases}0, & x>\frac{aA_1}{B_2-A_1},\\ 0, & x<\frac{aA_1}{B_2-A_1},\left(A_1-B_2\frac{x}{a+x}\right)x+y<\frac{P}{\theta},\\ -\frac{\beta_1}{a+x}<0, & x<\frac{aA_1}{B_2-A_1},\left(A_1-B_2\frac{x}{a+x}\right)x+y>\frac{P}{\theta}.\end{cases}$$

If $A_1\geq B_2$, it follows

$$G_{2_x}=\begin{cases}-\beta B_2\frac{2ax}{(a+x)^3}+(\beta_1A_1-h_2B_2)\frac{a}{(a+x)^2}, & \left(A_1-B_2\frac{x}{a+x}\right)x+y<\frac{P}{\theta},\\ -\frac{\beta_1}{\theta}\frac{P-\theta y}{(a+x)^2}-h_2B_2\frac{a}{(a+x)^2}<0, & \left(A_1-B_2\frac{x}{a+x}\right)x+y>\frac{P}{\theta}.\end{cases}$$

$$G_{2_y}=\begin{cases}0, & \left(A_1-B_2\frac{x}{a+x}\right)x+y<\frac{P}{\theta},\\ -\frac{\beta_1}{a+x}<0, & \left(A_1-B_2\frac{x}{a+x}\right)x+y>\frac{P}{\theta}.\end{cases}$$

Consider the case when

$$\begin{aligned}G_{2_x}&=-\beta B_2\frac{2ax}{(a+x)^3}+(\beta_1A_1-h_2B_2)\frac{a}{(a+x)^2}\\&=\frac{a(\beta_1A_1-2\beta_1B_2-h_2B_2)x+(\beta_1A_1-h_2B_2)a^2}{(a+x)^3}.\end{aligned}$$

Let $\tilde{x}=-\frac{(\beta_1A_1-h_2B_2)a}{\beta_1A_1-2\beta_1B_2-h_2B_2}$.

If $\beta_1A_1<h_2B_2$, then $\beta_1A_1-2\beta_1B_2-h_2B_2<0$ and $G_{2_x}<0$, $\forall(x,y)\in\Omega$.

If $\beta_1A_1>2\beta_1B_2+h_2B_2$, then $G_{2_x}>0$, $\forall(x,y)\in\Omega$.

If $h_2B_2<\beta_1A_1<2\beta_1B_2+h_2B_2$, then $G_{2_x}>0$, $\forall 0<x<\tilde{x}$, and $G_{2_x}<0$, $\forall x>\tilde{x}$.

Theorem 3.4. *The stability of internal equilibrium $E^*(x^*,y^*)$ follows that*

I When $x^*>\frac{aA_1}{B_2-A_1}$ with $A_1<B_2$, E^* is a saddle.

II When $x^*<\frac{aA_1}{B_2-A_1}$ and $(A_1-B_2\frac{x^*}{a+x^*})x^*+y^*<\frac{P}{\theta}$ with $A_1<B_2$; or $(A_1-B_2\frac{x^*}{a+x^*})x^*+y^*<\frac{P}{\theta}$ with $A_1>B_2$.

- *i If $\beta_1A_1<h_2B_2$, E^* is a saddle.*
- *ii If $\beta_1A_1>2\beta_1B_2+h_2B_2$, E^* is LAS if the producer nullcline is decreasing at E^*; otherwise, E^* is unstable.*
- *iii If $h_2B_2<\beta_1A_1<2\beta_1B_2+h_2B_2$. $\forall 0<x^*<\tilde{x}$, E^* is LAS if the producer nullcline is decreasing at E^*; otherwise, E^* is unstable. $\forall\tilde{x}<x^*$, E^* is a saddle.*

III $x^*<\frac{aA_1}{B_2-A_1}$ and $(A_1-B_2\frac{x^*}{a+x^*})x^*+y^*>\frac{P}{\theta}$ with $A_1<B_2$; or $(A_1-B_2\frac{x^*}{a+x^*})x^*+y^*>\frac{P}{\theta}$ with $A_1>B_2$. At E^*, if the slope of the grazer nullcline is less than that of the producer nullcline, then E^* is a saddle. Otherwise, E^* is LAS.

Proof. The Jacobian matrix of internal equilibrium $E^*(x^*,y^*)$ is

$$J_{E^*}=\begin{pmatrix}x^*F_{2_x}(x^*,y^*) & x^*F_{2_y}(x^*,y^*)\\ y^*G_{2_x}(x^*,y^*) & y^*G_{2_y}(x^*,y^*)\end{pmatrix}.$$

The trace and the determinant of J_{E^*} are given by

$$\begin{aligned}\mathrm{Tr}(J_{E^*})&=x^*F_{2_x}+y^*G_{2_y},\\ \mathrm{Det}(J_{E^*})&=x^*y^*(F_{2_x}G_{2_y}-F_{2_y}G_{2_x}).\end{aligned}$$

The slopes of the producer and grazer nullclines at (x,y) are defined by $-F_{2_x}/F_{2_y}$ and $-G_{2_x}/G_{2_y}$, respectively. We consider the following cases:

Case I: $x^*>\frac{aA_1}{B_2-A_1}$ with $A_1<B_2$.
At E^*, $G_{2_x}<0$, $G_{2_y}=0$ and $F_{2_y}<0$. Hence, $\mathrm{Det}(J_{E^*})<0$, i.e. E^* is a saddle.

Case II: $x^*<\frac{aA_1}{B_2-A_1}$ and $(A_1-B_2\frac{x^*}{a+x^*})x^*+y^*<\frac{P}{\theta}$ with $A_1<B_2$; or $(A_1-B_2\frac{x^*}{a+x^*})x^*+y^*<\frac{P}{\theta}$ with $A_1>B_2$.
At E^*, $G_{2_y}=0$, $F_{2_y}<0$ and $\mathrm{sign}(\mathrm{Tr}(J_{E^*}))=\mathrm{sign}(F_{2_x})=\mathrm{sign}\left(-\frac{F_{2_x}}{F_{2_y}}\right)$.

i If $\beta_1A_1<h_2B_2$, then $G_{2_x}<0$ and $\mathrm{Det}(J_{E^*})<0$. i.e. E^* is a saddle.

ii If $\beta_1A_1>2\beta_1B_2+h_2B_2$, then $G_{2_x}>0$ and $\mathrm{Det}(J_{E^*})>0$. Therefore, if the producer nullcline is decreasing at E^*, i.e. $-\frac{F_{2_x}}{F_{2_y}}<0$, then $\mathrm{Tr}(J_{E^*})<0$. It follows that E^* is LAS. Otherwise, E^* is unstable.

iii If $h_2B_2<\beta_1A_1<2\beta_1B_2+h_2B_2$, then for any $0<x^*<\tilde{x}$, $G_{2_x}>0$ and $\mathrm{Det}(J_{E^*})>0$. If the producer nullcline decreases at E^*, i.e. $-\frac{F_{2_x}}{F_{2_y}}<0$, then E^* is LAS; otherwise, E^* is unstable. $\forall x^*>\tilde{x}$, $G_{2_x}<0$ and $\mathrm{Det}(J_{E^*})<0$. Hence, E^* is a saddle.

Case III: $x^*<\frac{aA_1}{B_2-A_1}$ and $(A_1-B_2\frac{x^*}{a+x^*})x^*+y^*>\frac{P}{\theta}$ with $A_1<B_2$; or $(A_1-B_2\frac{x^*}{a+x^*})x^*+y^*>\frac{P}{\theta}$ with $A_1>B_2$.
At E^*, $G_{2_x}<0$, $G_{2_y}<0$ and $F_{2_y}<0$. It follows that

$$\begin{aligned}\mathrm{sign}(\mathrm{Det}(J_{E^*}))&=\mathrm{sign}(F_{2_x}G_{2_y}-G_{2_x}F_{2_y})\\&=\mathrm{sign}\left(\frac{F_{2_x}G_{2_y}-G_{2_x}F_{2_y}}{F_{2_y}G_{2_y}}\right)\\&=\mathrm{sign}\left(-\frac{G_{2_x}}{G_{2_y}}-\left(-\frac{F_{2_x}}{F_{2_y}}\right)\right).\end{aligned}$$

Therefore, at E^*, if the slope of the grazer nullcline is less than the slope of the producer nullcline, i.e., $-\frac{G_{2_x}}{G_{2_y}}<-\frac{F_{2_x}}{F_{2_y}}$, then $\mathrm{Det}(J_{E^*})<0$ and E^* is a saddle. Otherwise, if the slope of grazers is higher, i.e., $-\frac{G_{2_x}}{G_{2_y}}>-\frac{F_{2_x}}{F_{2_y}}$, then $\mathrm{Det}(J_{E^*})>0$, $F_{2_x}<0$, and $\mathrm{Tr}(J_{E^*})<0$. Hence, E^* is LAS. □

Two examples are provided to show the application of Theorem 3.4. For the first example, we choose $\beta_1=9.8$, $\beta_2=20$, $h_2=0.4$, $m_2=0.25$, $a_2=0.192$, $\sigma_1=0.001$, $\sigma_2=0.4$, $a=0.25$, $T=0.01$, $P=0.05$, and $K=1.85$. Rest parameters are shown in Table 2.1. It is easy to calculate that $A_1=0.9985<B_2=1.7285$. There are two internal equilibria denoted as E_2 and E_3, as shown in Fig. 1(a). $E_2(x_2,y_2)$ satisfies that $x_2<\frac{aA_1}{B_2-A_1}$ and $(A_1-B_2\frac{x_2}{a+x_2})x_2+y_2<\frac{P}{\theta}$. Furthermore, $\beta_1A_1=6.6149>2\beta_1B_2+h_2B_2=0.2292$. Therefore, as producer nullcline is increasing, based on Theorem 3.4 Case II, E_2 is unstable. $E_3(x_3,y_3)$ satisfies $x_3>\frac{aA_1}{B_2-A_1}$. Based on Theorem 3.4 case I, E_3 is a saddle. These conclusions are further approved by phase portrait in Fig. 1(b).

Another example is given as $h_2=0.4$, $m_2=0.25$, $\sigma_1=0.5$, $\sigma_2=0.4$, $a=0.25$, $T=0.01$, $P=0.05$ $K=1.85$. In this case, there are three internal equilibria denoted as E_2, E_3, and E_4, as shown in Fig. 2(a). E_2 satisfies that $(A_1-B_2\frac{x_2}{a+x_2})x_2+y_2<\frac{P}{\theta}$. Meanwhile, $A_1=0.6229>B_2=0.0017$ and $\beta_1A_1=0.3363>2\beta_1B_2+h_2B_2=0.0019$ hold. The producer nullcline is increasing at E_2. According to Theorem 3.4 case II, E_2 is unstable. On the other hand, E_3 and E_4 satisfies $(A_1-B_2\frac{x}{a+x})x+y>\frac{P}{\theta}$. At E_3 the slope of the producer nullcline is higher, while at E_4, the slope of the grazer is higher. By Theorem 3.4 case III, E_3 is a saddle and E_4 is LAS. These results align with simulation results in Fig. 2(b).

4. Numerical analysis

In this section, we employ numerical simulations to visually explore the impact of microplastics on aquatic population dynamics in both natural and laboratory settings separately.

4.1. The OMUF model

Here, we investigate the influence of microplastics using the OMUF model (3.5) and compare the differences between them under natural and laboratory settings. We set $a=0.0012$, $m_2=0.025$, $P=0.03$, and $K=2.5$ for all simulations. Bifurcation analysis is employed. Fig. 3(a) illustrates the bifurcation diagram over T for the system (3.5), where

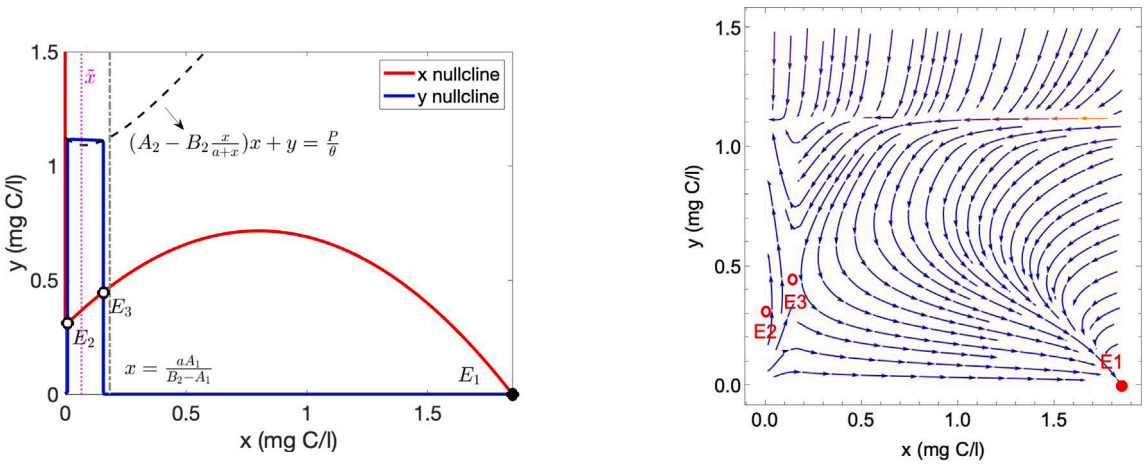

Fig. 1. (a) Nullclines of producers (x) and grazers (y) for system (3.8) for example 1. The red parabola-shaped curve is x-nullcline; the blue straight lines are y-nullclines. Two unstable equilibria E_2 and E_3 are highlighted as circles. (b) Corresponding phase portrait of system (3.8). E_2 is unstable and E_3 is a saddle.

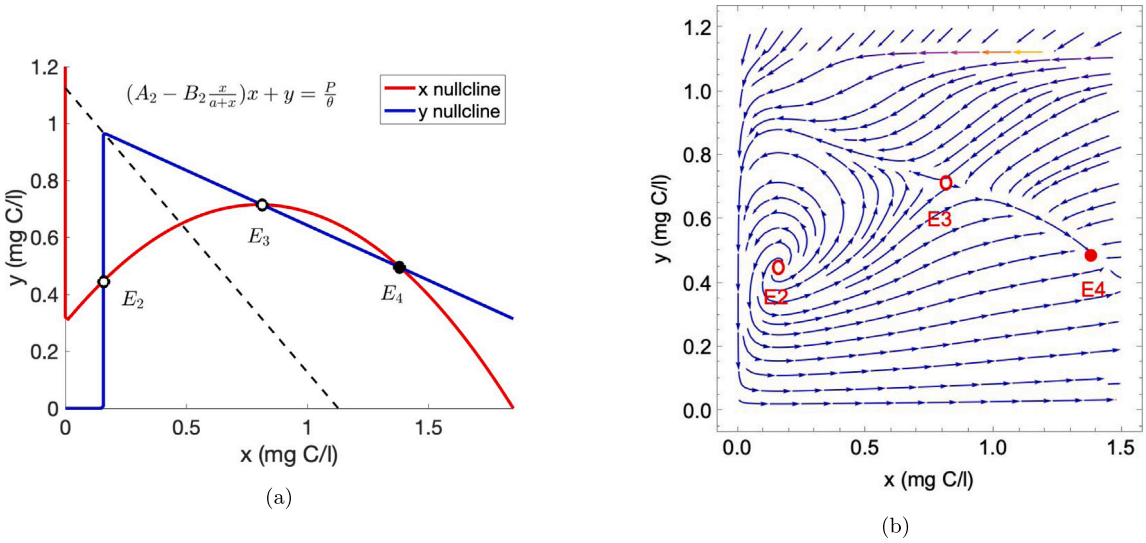

Fig. 2. (a) Nullclines of producers (x) and grazers (y) in system (3.8) for example 2. The x-nullcline is denoted by a red parabolic curve, and the y-nullclines are denoted by blue peaked lines. Unstable equilibria are marked with circles, and the stable equilibria are denoted by dots. (b) The corresponding phase portrait of system (3.8). E_2 is unstable, E_3 is a saddle point, and E_4 is stable.

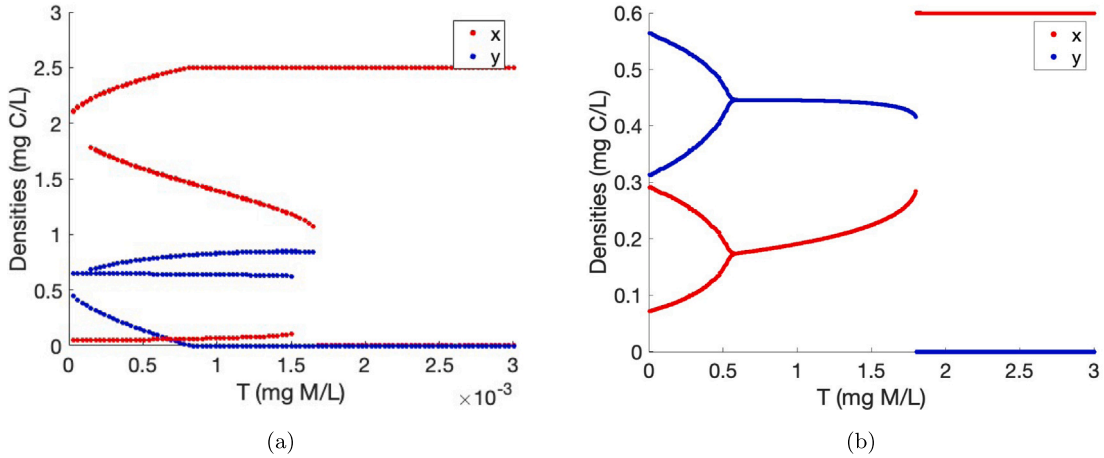

Fig. 3. Bifurcation diagram over varying microplastic concentration T. (a) OMUF model (3.5). (b) NM model (2.11).

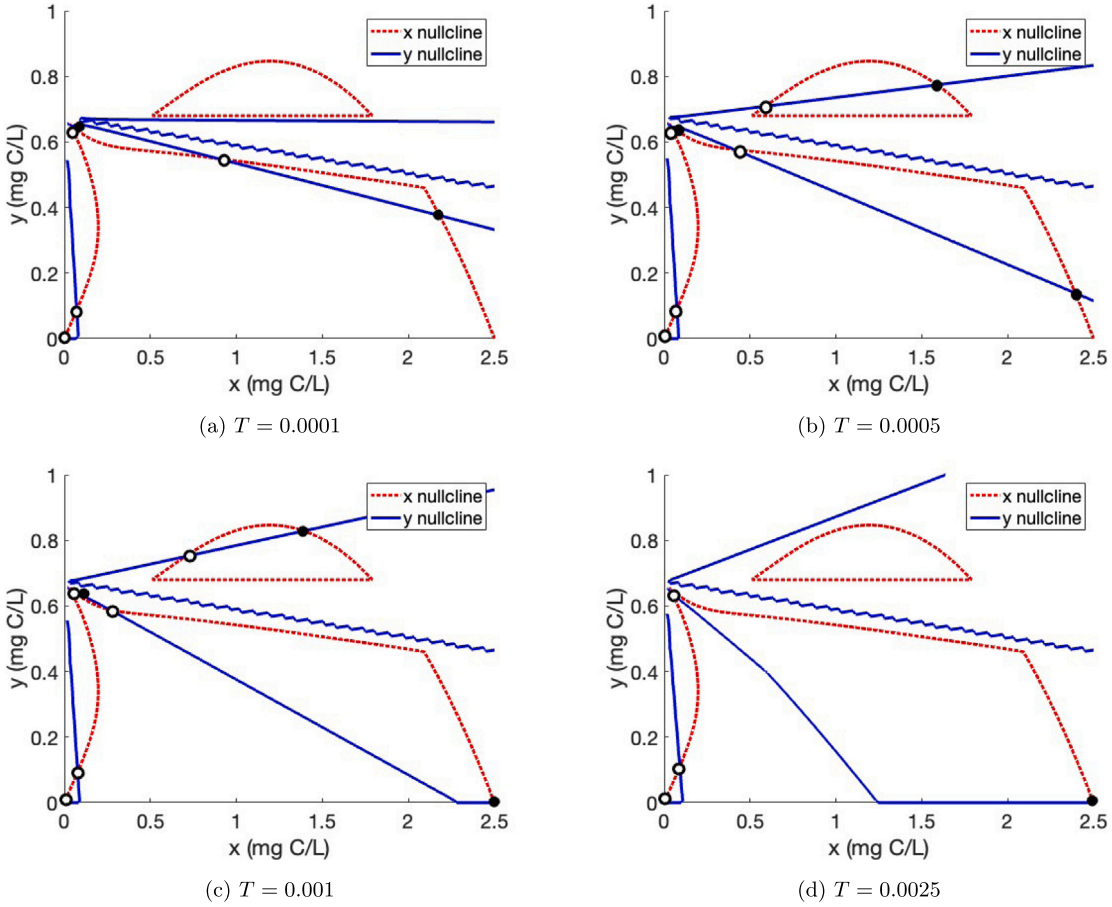

Fig. 4. Nullclines for system (3.5) under different microplastic concentration. (a) $T = 0.0001$, (b) $T = 0.0005$, (c) $T = 0.001$, (d) $T = 0.0025$. Red dashed curves represent the x-nullcline, while blue solid lines represent the y-nullclines. Unstable equilibria are marked with circles, and the stable equilibria are denoted by dots. Here we take $P = 0.03$, $K = 2.5$.

T represents the total microplastic concentration in the environment. Additionally, Fig. 4 displays the nullclines of producers and grazers.

The system (3.5) exhibits complicated dynamics. It admits a critical threshold at $T = 0.00165$, as illustrated in Fig. 3(a). When the microplastic concentration is higher than 0.000165, grazers go to extinction while producers stabilize at maximum carrying capacity K eventually, e.g., $T = 0.0025$ in Fig. 5(d). This aligns with that the producer-only equilibrium is the only stable equilibrium, as shown in Fig. 4(d).

However, when the microplastic concentration is below this threshold, the system displays diverse stability patterns. Specifically, when $T < 0.00015$, the system shows bistability. As demonstrated in 4(a) and Fig. 5(a), when $T = 0.0001$, there are five intersection points of the x-nullclines and y-nullclines, two of which are stable (denoted as black dots), while the remaining three are unstable (denoted as circles). In this case, the state of the system is highly dependent on the initial state. When $0.00015 < T < 0.00081$, the system (3.5) displays three stable states simultaneously. This is further supported by Figs. 4(b) and 5(b), when $T = 0.0005$, eight equilibria are present, with three of them being stable. Further increasing the microplastic concentration in the environment, the system still exhibits three stable states, while one of them is the producer-only state. An example is given when $T = 0.001$ in Figs. 4(c) and 5(c). This implies that if the initial grazer density is too low, although plenty of food is provided, grazers will still go to extinction. When $0.0015 < T < 0.00165$, the system again shows bistability with one stable boundary equilibrium.

The tolerance of the producer-grazer system described in (3.5) to microplastics is significantly lower, compared to that of the system defined in (2.11), as demonstrated in Fig. 3. This implies that producers and grazers are more sensitive to microplastics in natural environments. This heightened sensitivity can be attributed to various challenges such as food scarcity, predation risk, exposure to multiple toxins, and human disruptions. All of these challenges increase the predation difficulty and vulnerability of grazers. Interestingly, under natural conditions for grazers, species tend to exhibit multiple stability, while at most one stable state is observed for the NM model.

4.2. The NM model

In this section, we try to investigate the effect of light, microplastics, and nutrients on the population dynamics respectively through NM model (2.11). For a simple Holling type II functional response, we take $c = 0.81$, $a = 0.25$, $m_2 = 0.25$ in this section (Anderson et al., 2015). Fig. 7 shows the comparison between two different total phosphorus $P = 0.023$ and $P = 0.05$. K implies the light intensity, which influences the quality and quantity of food for grazers. Fig. 7(a) and 7(b) illustrate how densities of producers and grazers vary when the light intensity and microplastic concentration vary. Figs. 7(c) and 7(d) show the corresponding two parameters bifurcation diagrams. In Region II (black), the system admits a limit cycle; in Region I (red), the system admits a stable coexistence state; in Region III (blue), the system admits a producer-only state. Figs. 7(e) and 7(f) show the two bifurcation diagrams for grazer production efficiency function, i.e. $e(v)$, illustrating the main limitation for their growth. Red dots indicate the nutrient is the main limitation; Blue dots indicate the microplastics are the main limitation for grazers. Figs. 7(g) and 7(h) shows the body burdens for $P = 0.023$ and $P = 0.05$, respectively.

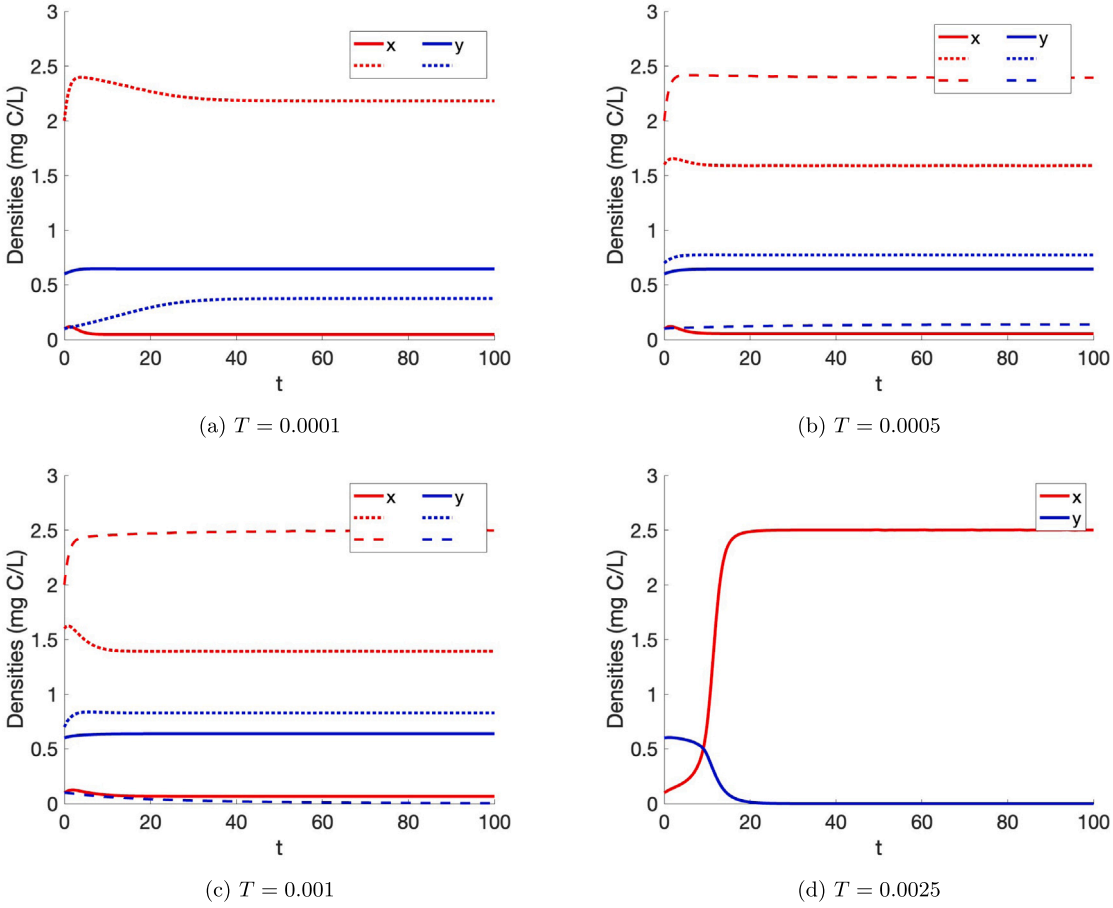

(a) $T = 0.0001$ (b) $T = 0.0005$

(c) $T = 0.001$ (d) $T = 0.0025$

Fig. 5. Time series for system (3.5). (a) $T = 0.0001$, (b) $T = 0.0005$, (c) $T = 0.001$, (d) $T = 0.0025$. Different types of curves indicate solutions with different initial values.

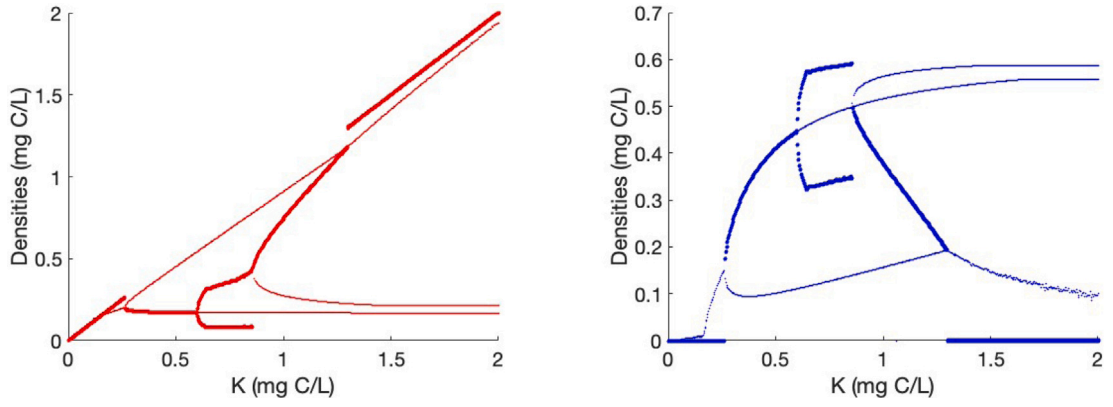

(a) Producers (b) Grazers

Fig. 6. Bifurcation diagram for varying light level K for system (2.11).

4.2.1. *Influence of light intensity*

Referring to Figs. 7(c) and 7(d), we observe that grazers cannot survive when the light intensity is either too low or too high. Optimal survival conditions occur within a moderate range of light intensity, benefiting both producers and grazers. To gain deeper insights into how light intensity influences population dynamics, we employ bifurcation analysis over the parameter K. Fig. 6 provides an example when $P = 0.023$, $T = 0.05$. The corresponding time series of the solution is presented in Fig. 8.

When the light intensity is extremely low ($K < 0.268$), producer growth is severely constrained due to insufficient photosynthesis, resulting in low producer density. Consequently, grazers face extinction due to food scarcity. An example with $K = 0.1$ is illustrated in Fig. 8(a). Within the moderate range of light intensity ($0.268 < K < 1.296$), producers and grazers find a balance for coexistence. Specifically, when $0.268 < K < 0.596$, the system maintains a stable coexistence state, exemplified by $K = 0.4$ in Fig. 8(b). At $K = 0.596$, a Hopf bifurcation occurs. With further increases in light intensity, the densities of producers and grazers oscillate periodically, as demonstrated by $K = 0.8$

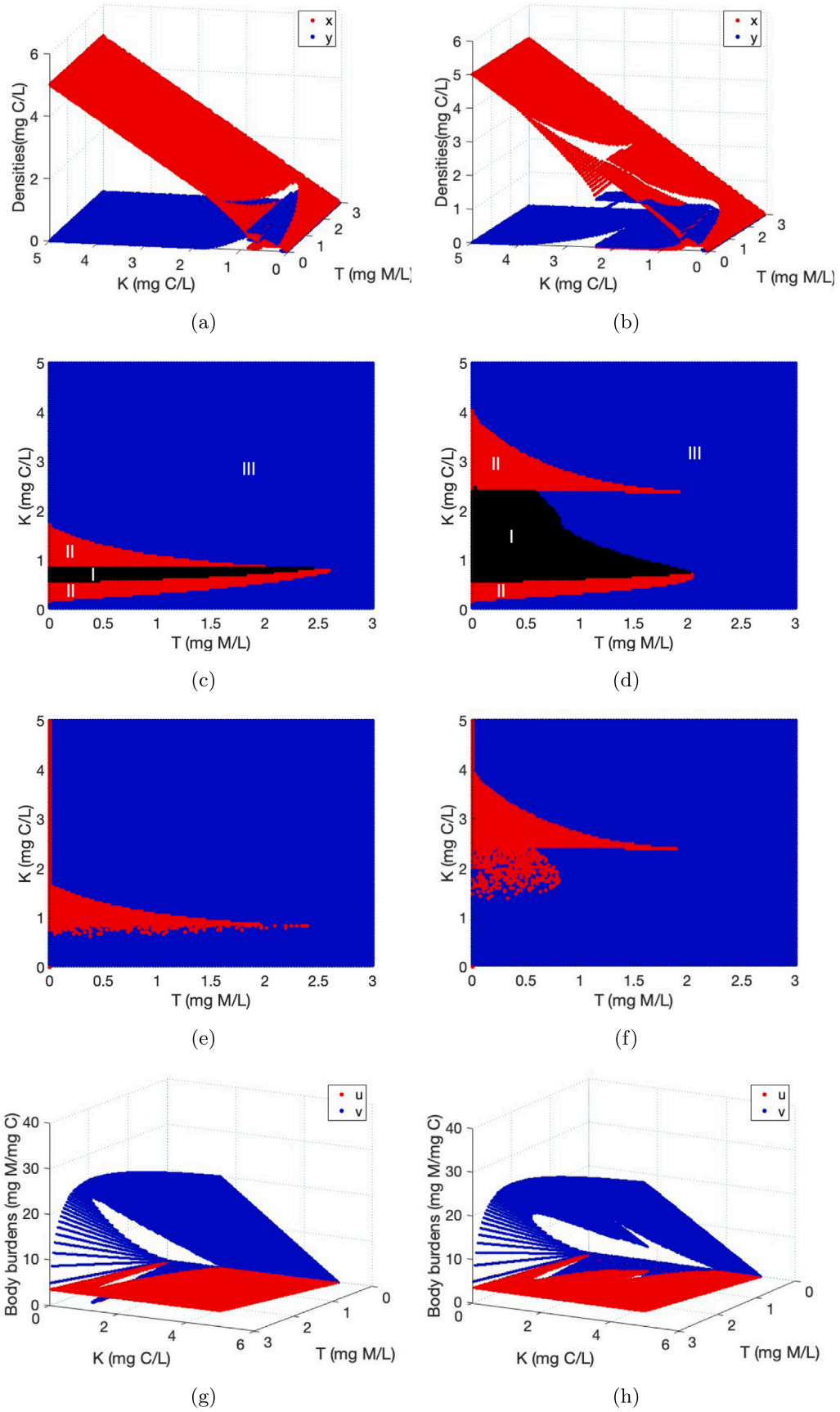

Fig. 7. (a)(b) 3D phase portraits of (2.11). (c)(d) Bifurcation diagrams for light intensity K and microplastic concentration T. (e)(f) Main limitation on grazer growth rate. (g)(h) Microplastic body burdens for producers and grazers. For the panels on the left, we choose $P = 0.023$, and for the panels on the right, we choose $P = 0.05$.

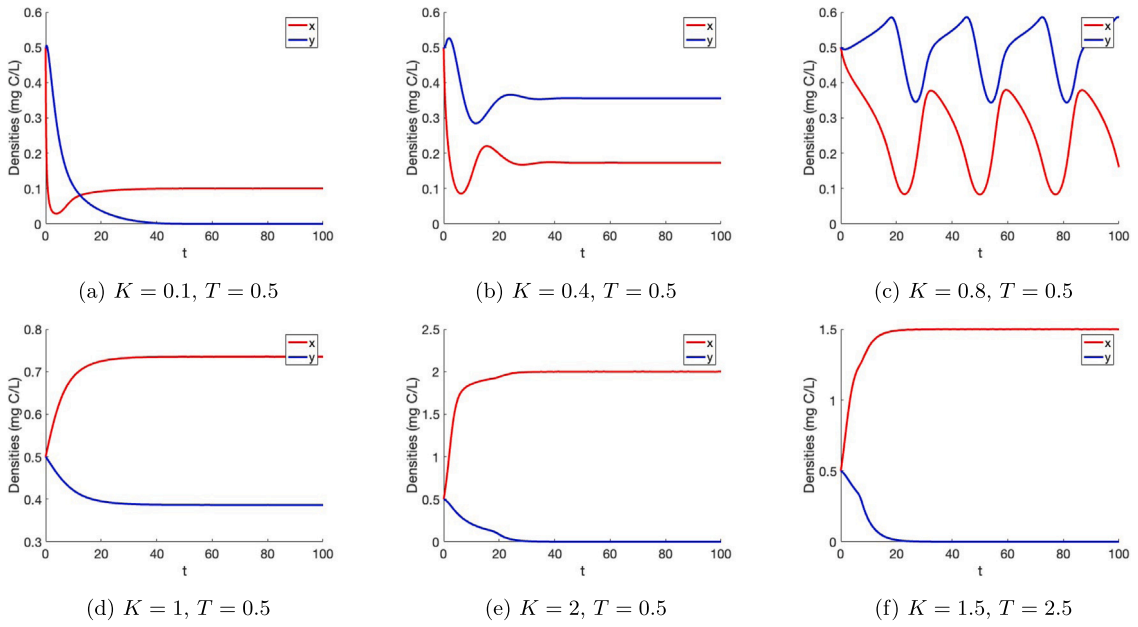

(a) $K = 0.1$, $T = 0.5$ (b) $K = 0.4$, $T = 0.5$ (c) $K = 0.8$, $T = 0.5$

(d) $K = 1$, $T = 0.5$ (e) $K = 2$, $T = 0.5$ (f) $K = 1.5$, $T = 2.5$

Fig. 8. Time series of producers and grazers in system (2.11) with $P = 0.023$.

in Fig. 8(c). At $K = 0.856$, another Hopf bifurcation happens, and the system transitions to a stable state again, e.g., $K = 1$ in Fig. 8(d). Higher light intensity typically indicates stronger photosynthesis, which promotes producer growth. However, with an abundance of carbon, the P:C ratio in producers decreases, indicating a decline in food quality for grazers. When light intensity becomes excessively strong, the low-quality food becomes insufficient to support the survival of grazers, ultimately leading to their extinction. This scenario is depicted in Fig. 8(e) with $K = 2$.

4.2.2. Influence of microplastics

From Fig. 7(a)–7(d), it is evident that when the concentration of microplastics in the environment becomes excessively high ($T > 1.8$), grazers are unable to survive. Fig. 8(f) provides an example when $T = 2.5$ for the case $P = 0.23$. However, when the density of microplastics remains within a reasonable range, both producers and grazers have an opportunity to coexist. We conduct a bifurcation analysis over T, using moderate light intensity ($K = 0.7$) as an example, as illustrated in Fig. 3(b). When microplastic concentration is low ($T < 0.57$), the system (2.11) admits a limit cycle. Further increasing microplastic concentration, producers and grazers can coexist stably.

Low light intensity and a low nutrient level naturally limit the growth of producers and grazers, even without the presence of microplastics. However, the existence of microplastics amplifies this limitation imposed by light intensity and nutrient availability. The upper boundary of the top region II decreases, and the lower boundary of the bottom region II increases when parameter T rises, as shown in Figs. 7(c) and 7(d). This indicates that as the concentration of microplastics in the environment increases, the system exhibits reduced resistance to low light intensity and nutrient-poor conditions. For example, consider the case of $P = 0.023$. When $T = 0$ (no microplastics), a relatively low light intensity of $K = 0.185$ is enough to support the survival of grazers, as shown in Fig. 7(c). However, when $T = 0.5$, the producer-grazer system requires a higher minimum light intensity of $K = 0.26$ to maintain coexistence, as depicted in Fig. 6(b).

High levels of microplastics in the environment do not always correspond to high body burdens in organisms. As seen in Fig. 7(g) and 7(h), in general, an increase in the toxin concentration in the environment leads to higher body burdens in both producers and grazers. However, when food nutrients are abundant, and light intensity is moderate, the body burdens remain at a low level even with increasing levels of microplastics in the environment. This observation potentially explains why, in most experiments, the inhibition effects on grazer growth show a positive correlation with the total abundance of microplastics in the environment, whereas in some experiments, their relationship is not strictly positive (Canniff and Hoang, 2018).

Grazers exhibit greater sensitivity to microplastics, compared to producers. As depicted in Figs. 7(g) and 7(h), the body burdens in producers consistently remain at relatively low levels when light intensity and microplastic concentration vary, whereas the body burdens in grazers can reach significantly higher values. When the body burdens in grazers become excessively high, they face the risk of extinction, as illustrated in Fig. 8(a), Fig. 8(e), Fig. 8(f), Fig. 9(a), Fig. 9(e), and Fig. 9(f). Moreover, the stability of producers and grazers is significantly influenced by their body burdens. For instance, the densities of producers and grazers remain stable when their body burdens exhibit stability, as observed in Fig. 8(b), Fig. 8(d), Fig. 9(b), and Fig. 9(d). Conversely, when their body burdens oscillate periodically, both producers and grazers experience oscillations in their populations, as exemplified in Figs. 8(c) and 9(c).

In the case where producers can utilize microplastics for their growth, we set $\alpha_2 = -0.09$, $P = 0.05$, and $\sigma_1 = 0.6$. This results in a coexistence area that is more than three times larger than that shown in Fig. 7(d), as illustrated in Fig. 10. This implies that the producer-grazer system shows higher resistance to microplastics. In particular, the maximum microplastic concentration that allows the survival of both producers and grazers is 4.5, which is significantly higher than that shown in Fig. 7(d).

4.2.3. Influence of nutrient

As the total phosphorus concentration in the environment (i.e. P) increases, the producer-grazer system exhibits greater resistance to intense light conditions. For instance, when $P = 0.023$, the maximum light intensity that can be utilized to sustain the coexistence of both

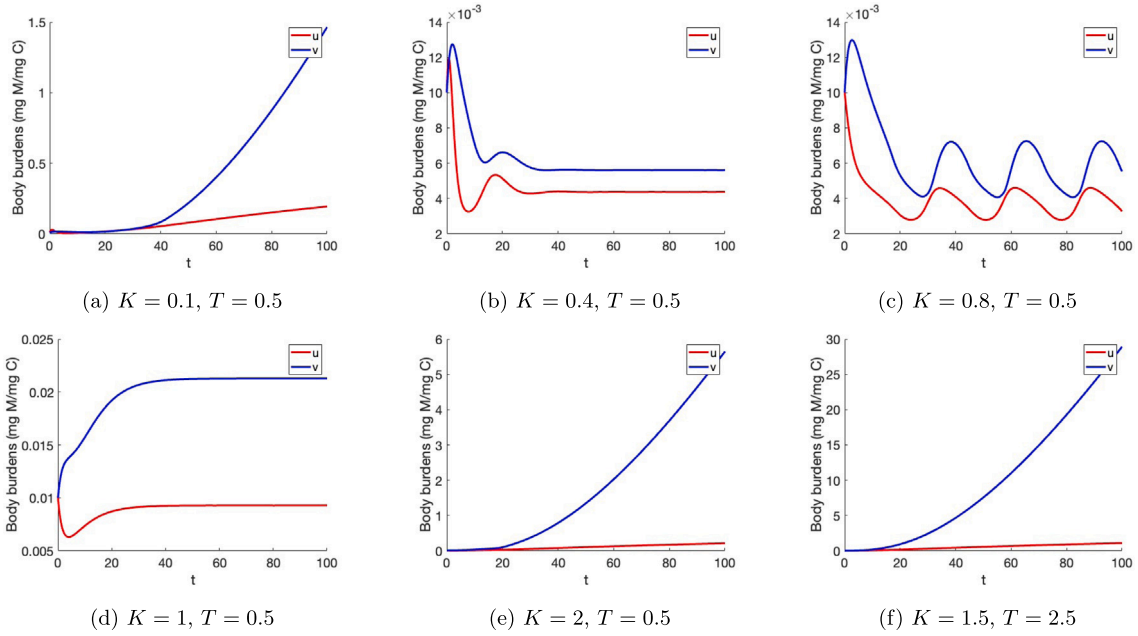

Fig. 9. Time series of microplastic body burdens of producers and grazers in system (2.11) with $P = 0.023$.

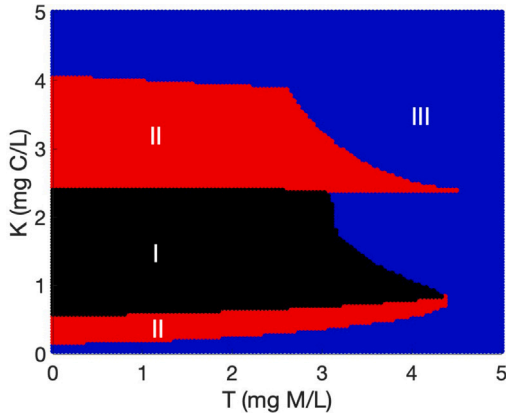

Fig. 10. Two-parameter bifurcation diagram for varying light level K and microplastics level T for system (2.11). Here we take $\sigma_1 = 0.6$, $\alpha_2 = -0.09$.

producers and grazers is 1.66, as illustrated in Fig. 7(c). However, when $P = 0.05$, this maximum light intensity increases to 4.05, as shown in Fig. 7(d). This phenomenon occurs because higher light intensity typically leads to increased producer density. With more carbon available, the producer's P:C ratio decreases, meaning that the nutrient level in producers decreases. When the nutrient level falls below the grazers' demand threshold, grazers go extinct. When the total phosphorus concentration in the environment is low, even moderate light intensity can lead to low nutrient levels in producers, making it difficult for grazers to survive. However, as the total phosphorus concentration in the environment increases, high light intensity can still ensure that the nutrient levels in producers remain at a moderate level, which is sufficient to support the survival of grazers.

Grazers can survive only when their body burdens of microplastics are relatively low as discussed in Section 4.2.2. However, the main limitation for the growth of grazers is not always the same. When the light intensity is low, the nutrient level in producers is sufficient, their microplastic body burdens become the primary limiting factor. As light intensity increases, the nutrient level in producers decreases. Consequently, the primary limitation to grazer growth transitions to inadequate nutrients gradually, as shown in Figs. 7(e) and 7(f).

5. Discussion

Microplastics can be mistakenly ingested or adhere to the surfaces of marine organisms, resulting in significant adverse effects (Zhang et al., 2017; Liu et al., 2019; Sazli et al., 2023; Gregory, 1996; Derraik, 2002; Blarer and Burkhardt-Holm, 2016; Alomar et al., 2017). This paper presents two stoichiometric models to investigate population dynamics in the presence of microplastics in both field and laboratory settings. The interactive effects of light, nutrients, and microplastics on population dynamics have been rigorously studied.

For natural ecosystems, the OMUF model reveals complex dynamics. When the microplastic concentration is relatively low, the behavior of the system is strongly influenced by the initial conditions and can exhibit bistability or tristability. Conversely, when microplastics in the environment become excessively abundant, the only outcome is the extinction of grazers. Furthermore, the tolerance to microplastics of the producer-grazer system described in OMUF model (3.5) is significantly lower, compared to that of the system defined in NM model (2.11). This discrepancy potentially arises from the fact that in the natural ecosystem, grazers have to face more challenges and pay significant feeding costs, such as food scarcity, nutrient deficiencies, predation risk, multiple toxins, and human impact, making them more susceptible to microplastics.

Extreme light condition, either too low or too high, restricts the growth of grazers. When light intensity is excessively low, producers can only survive at low densities due to weakened photosynthesis, and grazers go extinct because of insufficient food. When light intensity is excessively high, the P:C ratio in producers becomes very low, and grazers go extinct due to nutrient deficiency. However, when light intensity falls within a moderate range, coexistence of both species may occur, and the system demonstrates a greater ability to withstand microplastics.

The populations of producers and grazers are highly impacted by the concentration of microplastics. Grazers prove to be more vulnerable to microplastics compared to producers. High microplastic concentrations lead to the extinction of grazers, while producers can persist even in

the presence of extremely high microplastic levels. This aligns with the stability analysis in Theorem 3.2 that the system will never fully collapse. In cases where producers can utilize microplastics for growth, the system shows much greater resilience to microplastics.

Intuitively, high environmental microplastic levels imply elevated microplastic body burdens in organisms, but this is not always true. In most situations, higher environmental microplastic concentrations result in increased body burdens for producers and grazers. However, when nutrients are plentiful and light is moderate, their body burdens remain low despite increasing environmental microplastics. This may explain why, in some experiments, the mortality rate or growth inhibition is not positively correlated with microplastic concentration (Canniff and Hoang, 2018).

The influence of light intensity, nutrients, and microplastics on population dynamics is highly intertwined. When light intensity is relatively low, the primary limitation on the growth of grazers is microplastic body burdens, while with high light intensity, their growth is primarily constrained by food quality. Increasing phosphorus concentration in the environment enhances the resistance of the producer-grazer system to intense light conditions. Conversely, the presence of microplastics amplifies the constraints on grazer growth related to food quality and quantity imposed by excessively low or high light intensities. Moreover, as the concentration of microplastics in the environment rises, the system demonstrates decreased resilience to food and nutrient discrepancy conditions.

The models developed here primarily focus on producer-grazer dynamics. However, the transfer of microplastics through multiple trophic interactions can significantly affect the trophic cascade strength and stability of plankton ecosystems (Pan et al., 2022; Lu et al., 2016). Considering a higher-dimensional food chain model in the future could provide further insights. Additionally, beyond their impact on population growth, microplastics can also influence the behavior and personality of individual organisms (Bhuyan, 2022; Chen et al., 2022), such as the boldness and shyness of fish. Investigating these effects on the personality of organisms could be an intriguing avenue for future research. Furthermore, the impact of microplastics is closely related to particle size (Wu et al., 2021; Gray and Weinstein, 2017). Organisms may show opposite responses to various sizes of microplastics, and the underlying mechanisms are complicated (Yokota et al., 2017; Mao et al., 2018; Jiao et al., 2022; Canniff and Hoang, 2018; Cui et al., 2017; Duis and Coors, 2016; Nolte et al., 2017; Zhang et al., 2017; Khoironi et al., 2019; Sjollema et al., 2016; Besseling et al., 2014). Therefore, incorporating different microplastic sizes into future models is expected to be helpful for better understanding the mechanism of how microplastics influence aquatic ecosystem dynamics.

CRediT authorship contribution statement

Tianxu Wang: Formal analysis, Software, Validation, Visualization, Writing – original draft. **Hao Wang:** Conceptualization, Data curation, Funding acquisition, Investigation, Methodology, Project administration, Supervision, Validation, Writing – review & editing.

Declaration of competing interest

The authors declare that they have no known competing financial interests or personal relationships that could have appeared to influence the work reported in this paper.

Acknowledgments

The research of Hao Wang was partially supported by the Natural Sciences and Engineering Research Council of Canada (Individual Discovery Grant RGPIN-2020-03911 and Discovery Accelerator Supplement Award RGPAS-2020-00090) and the Canada Research Chairs program (Tier 1 Canada Research Chair Award).

Appendix. Parameters

(a) α_2 is estimated by

$$\alpha_2(\text{mg C/mg M}) = \frac{\text{Decrease of algae density (mg C/L)}}{\text{Microplastic concentration (mg M/L)}}.$$

The reduction in algae optical density (OD_{680}) ranges from 0.05 to 0.48 across various categories of 100 mg/L microplastics (Yang et al., 2020). The relationship between (mg C/L) and (OD_{680}) is expressed as follows (Lavrinovičs et al., 2021):

$$(\text{mg C/L}) = 1000(0.4076 \times (OD_{680}) - 0.0052).$$

Therefore,

$$\alpha_{2\max} = \frac{1000(0.4076 \times 0.48 - 0.0052)}{100} = 1.9$$
$$\alpha_{2\min} = \frac{1000(0.4076 \times 0.05 - 0.0052)}{100} = 0.152$$

The parameter α_2 can also be deduced using the four-day algae density data in Zhang et al. (2017). Considering a cell density of skeletonema costatum at 10^{-8} mg/cell, α_2 is estimated as -0.0989 as in Fig. 11(a). Consequently, we consider α_2 to fall within the range of -0.0989 to 1.9.

(b) β_2 is estimated as

$$\beta_2(\text{mg C/mg M}) = \frac{\text{Decrease of neonate density (mg C/L)}}{\text{Microplastic concentration (mg M/L)}}.$$

The reduction in the count of neonates varies from 3 to 73 under diverse light conditions and microplastic concentrations (Guilhermino et al., 2021). The dry weight of the Daphnia neonate is estimated as 0.002 mg/individual. Then by fitting data, we obtain $8.7 < \beta_2 < 15.78$, as shown in Fig. 11(b).

(c) h_2 is estimated as

$$h_2(\text{mg C/mg M/day}) = \frac{\frac{\text{Density of death neonate (mg C/L)}}{\text{Microplastic concentration (mg M/L)}}}{\text{Experiment time (day)}}.$$

Based on data in Guilhermino et al. (2021), $0.11 < h_2 < 0.29$.

(d) a_1 is estimated by

$$a_1(\text{L/mg C/day}) = \frac{\frac{\frac{\text{Uptake microplastic concentration (mg C/L)}}{\text{Total microplastic concentration (mg C/L)}}}{\text{Algae density (mg C/L)}}}{\text{Experiment time (day)}}.$$

According to Bhattacharya et al. (2010), the uptake rate (adsorption and absorption capacities) for positively and negatively charged nanoparticles are approximately 7/8 and 3/8, respectively. Algae density is considered equivalent to microplastic concentration. This leads to a range of $0.0056 < a_1 < 0.0131$.

(e) Assume the dry weight of one daphnia is 0.179 mg (Simčič and Anton, 1997), then the density of 10 daphnia in 50 ml media is given by

$$\frac{10 * 0.178}{50 * 10^{-3}} = 35.6 \quad (\text{mg C/L}).$$

b_1 is estimated as

$$b_1(\text{L/mg C/day}) = \frac{\frac{\text{Mean number particles counted inside Daphnia per day}}{\text{Mean number particles counted in Water per day}}(1/\text{day})}{\text{Density of Daphnia(mg C/L)}}.$$

Utilizing the data from Elizalde-Velázquez et al. (2020), the values for b_1 are determined as follows:

For high concentration exposure: $b_1 = \frac{0.034}{35.6} = 0.00096$.

For low concentration exposure: $b_1 = \frac{0.026}{35.6} = 0.00073$.

Therefore, the range of b_1 is set to be 0.00073 to 0.00096.

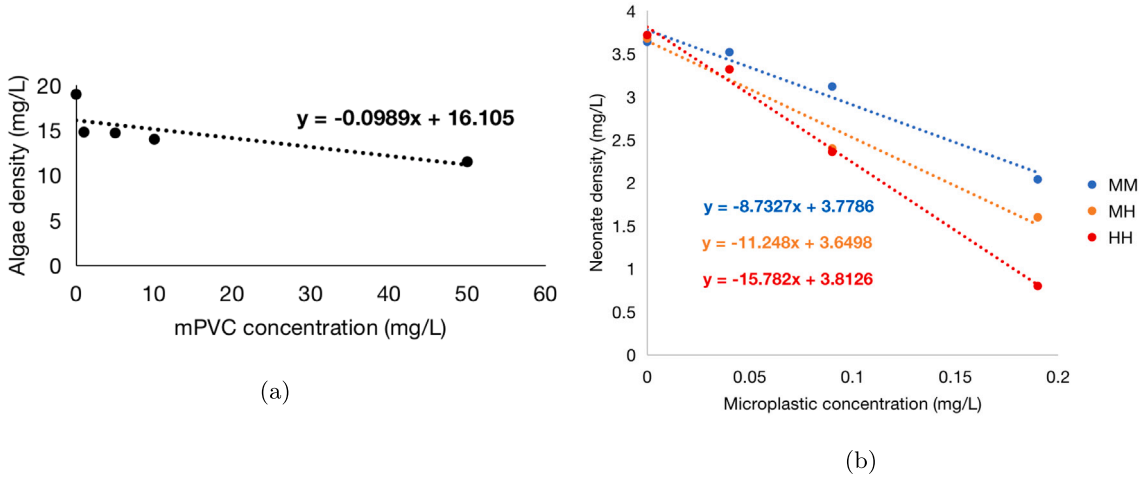

Fig. 11. (a) Data of algae density under various microplastic concentrations from (Yang et al., 2020). (b) Data of neonate density under different light and temperature conditions from Guilhermino et al. (2021). "MM" represents 20 °C with moderate light intensity, "MH" represents 20 °C with high light intensity, and "HH" represents 25 °C with high light intensity.

References

Alomar, Carme, Sureda, Antoni, Capó, Xavier, Guijarro, Beatriz, Tejada, Silvia, Deudero, Salud, 2017. Microplastic ingestion by Mullus surmuletus Linnaeus, 1758 fish and its potential for causing oxidative stress. Environ. Res. 159, 135–142.

Andersen, Tom, 2013. Pelagic Nutrient Cycles: Herbivores As Sources and Sinks. vol. 129, Springer Science & Business Media.

Anderson, A., Andrady, A., Arthur, C., Baker, J., Bouwman, H., Gall, S., Hildalgo-Ruz, V., Köhler, A., Lavender Law, K., Leslie, H.A., et al., 2015. Sources, fate and effects of microplastics in the environment: a global assessment. GESAMP Rep. Stud. Ser. (90).

Bertram, P.E., Hart, B.A., 1979. Longevity and reproduction of Daphnia pulex (de Geer) exposed to cadmium-contaminated food or water. Environ. Pollut. (1970) 19 (4), 295–305.

Besseling, Ellen, Wang, Bo, Lurling, Miquel, Koelmans, Albert A., 2014. Nanoplastic affects growth of S. obliquus and reproduction of D. magna. Environ. Sci. Technol. 48 (20), 12336–12343.

Bhattacharya, Priyanka, Lin, Sijie, Turner, James P., Ke, Pu Chun, 2010. Physical adsorption of charged plastic nanoparticles affects algal photosynthesis. J. Phys. Chem. C 114 (39), 16556–16561.

Bhuyan, Md Simul, 2022. Effects of microplastics on fish and in human health. Front. Environ. Sci. 10, 250.

Blarer, Pascal, Burkhardt-Holm, Patricia, 2016. Microplastics affect assimilation efficiency in the freshwater amphipod Gammarus fossarum. Environ. Sci. Pollut. Res. 23, 23522–23532.

Canniff, Patrick M., Hoang, Tham C., 2018. Microplastic ingestion by daphnia magna and its enhancement on algal growth. Sci. Total Environ. 633, 500–507.

Cao, Qingsheng, Sun, Wenbo, Yang, Tian, Zhu, Zhu, Jiang, Yinan, Hu, Wenlong, Wei, Wenzhi, Zhang, Yingying, Yang, Hui, 2022. The toxic effects of polystyrene microplastics on freshwater algae chlorella pyrenoidosa depends on the different size of polystyrene microplastics. Chemosphere 308, 136135.

Carbery, Maddison, O'Connor, Wayne, Palanisami, Thavamani, 2018. Trophic transfer of microplastics and mixed contaminants in the marine food web and implications for human health. Environ. Int. 115, 400–409.

Chae, Yooeun, Kim, Dasom, An, Youn-Joo, 2019. Effects of micro-sized polyethylene spheres on the marine microalga Dunaliella salina: Focusing on the algal cell to plastic particle size ratio. Aquat. Toxicol. 216, 105296.

Chen, Ming, Fan, Meng, Kuang, Yang, 2017. Global dynamics in a stoichiometric food chain model with two limiting nutrients. Math. Biosci. 289, 9–19.

Chen, Yuling, Li, Weiwei, Xiang, Lingli, Mi, Xiangyuan, Duan, Ming, Wu, Chenxi, 2022. Fish personality affects their exposure to microplastics. Ecotoxicol. Environ. Saf. 233, 113301.

Cui, Rongxue, Kim, Shin Woong, An, Youn-Joo, 2017. Polystyrene nanoplastics inhibit reproduction and induce abnormal embryonic development in the freshwater crustacean Daphnia galeata. Sci. Rep. 7 (1), 12095.

De Luna, J.T., Hallam, T.G., 1987. Effects of toxicants on populations: a qualitative approach IV. Resource-consumer-toxicant models. Ecol. Model. 35 (3–4), 249–273.

Derraik, José G.B., 2002. The pollution of the marine environment by plastic debris: a review. Mar. Pollut. Bull. 44 (9), 842–852.

Duis, Karen, Coors, Anja, 2016. Microplastics in the aquatic and terrestrial environment: sources (with a specific focus on personal care products), fate and effects. Environ. Sci. Eur. 28 (1), 1–25.

Eerkes-Medrano, Dafne, Thompson, Richard C., Aldridge, David C., 2015. Microplastics in freshwater systems: a review of the emerging threats, identification of knowledge gaps and prioritisation of research needs. Water Res. 75, 63–82.

EFSA Panel on Contaminants in the Food Chain (CONTAM), 2016. Presence of microplastics and nanoplastics in food, with particular focus on seafood. Efsa J. 14 (6), e04501.

Elizalde-Velázquez, Armando, Carcano, Analicia M., Crago, Jordan, Green, Micah J., Shah, Smit A., Cañas-Carrell, Jaclyn E., 2020. Translocation, trophic transfer, accumulation and depuration of polystyrene microplastics in Daphnia magna and Pimephales promelas. Environ. Pollut. 259, 113937.

Ferguson, Matthew D., 2011. The influence of humic acid and water hardness on the partitioning of silver ions and nanoparticles between fresh water and freshwater algae.

Fossi, Maria Cristina, Panti, Cristina, Guerranti, Cristiana, Coppola, Daniele, Giannetti, Matteo, Marsili, Letizia, Minutoli, Roberta, 2012. Are baleen whales exposed to the threat of microplastics? A case study of the Mediterranean fin whale (Balaenoptera physalus). Mar. Pollut. Bull. 64 (11), 2374–2379.

Freedman, H.I., Shukla, J.B., 1991. Models for the effect of toxicant in single-species and predator-prey systems. J. Math. Biol. 30 (1), 15–30.

Gall, Sarah C., Thompson, Richard C., 2015. The impact of debris on marine life. Mar. Pollut. Bull. 92 (1–2), 170–179.

Gašparovic, Blazenka, Vrana, Ivna, Frka, Sanja, Pfannkuchen, Daniela Maric, Vlašicek, Ivan, Djakovac, Tamara, Ivancic, Ingrid, Tankovic, Mirta Smodlaka, Milinkovic, Andrea, Flanjak, Lana, et al., 2023. Paradox of relatively more phospholipids in phytoplankton in phosphorus limited sea. Limnol. Oceanogr. 9999, 1–14.

Ghosh, M., Chattopadhyay, N.R., 2005. Effects of carbon/nitrogen/phosphorus ratio on mineralizing bacterial population in aquaculture systems. J. Appl. Aquac. 17 (2), 85–98.

Goldstein, Miriam C., Goodwin, Deborah S., 2013. Gooseneck barnacles (Lepas spp.) ingest microplastic debris in the North Pacific Subtropical Gyre. PeerJ 1, e184.

Gray, Austin D., Weinstein, John E., 2017. Size-and shape-dependent effects of microplastic particles on adult daggerblade grass shrimp (Palaemonetes pugio). Environ. Toxicol. Chem. 36 (11), 3074–3080.

Gregory, Murray R., 1996. Plastic 'scrubbers' in hand cleansers: a further (and minor) source for marine pollution identified. Mar. Pollut. Bull. 32 (12), 867–871.

Guilhermino, Lúcia, Martins, Alexandra, Cunha, Sara, Fernandes, José O., 2021. Long-term adverse effects of microplastics on Daphnia magna reproduction and population growth rate at increased water temperature and light intensity: Combined effects of stressors and interactions. Sci. Total Environ. 784, 147082. http://dx.doi.org/10.1016/j.scitotenv.2021.147082, URL https://www.sciencedirect.com/science/article/pii/S0048969721021525.

Hallam, T.G., Clark, C.E., Jordan, G.S., 1983a. Effects of toxicants on populations: a qualitative approach II. First order kinetics. J. Math. Biol. 18, 25–37.

Hallam, T.G., Clark, C.E., Lassiter, R.R., 1983b. Effects of toxicants on populations: a qualitative approach I. Equilibrium environmental exposure. Ecol. Model. 18 (3–4), 291–304.

Hecky, R.E., Kilham, Peter, 1988. Nutrient limitation of phytoplankton in freshwater and marine environments: a review of recent evidence on the effects of enrichment 1. Limnol. Oceanogr. 33 (4part2), 796–822.

Hoffschroeer, Nadine, Grassl, Niklas, Steinmetz, Arne, Sziegoleit, Lukas, Koch, Marita, Zeis, Bettina, 2021. Microplastic burden in Daphnia is aggravated by elevated temperatures. Zoology 144, 125881.

Hu, Lingling, Su, Lei, Xue, Yingang, Mu, Jingli, Zhu, Jingmin, Xu, Jiang, Shi, Huahong, 2016. Uptake, accumulation and elimination of polystyrene microspheres in tadpoles of Xenopus tropicalis. Chemosphere 164, 611–617.

Huang, Qihua, Parshotam, Laura, Wang, Hao, Bampfylde, Caroline, Lewis, Mark A., 2013. A model for the impact of contaminants on fish population dynamics. J. Theoret. Biol. 334, 71–79.

Huang, Qihua, Wang, Hao, Lewis, Mark A., 2015. The impact of environmental toxins on predator–prey dynamics. J. Theoret. Biol. 378, 12–30.

Jeyasingh, Punidan D., Goos, Jared M., Thompson, Seth K., Godwin, Casey M., Cotner, James B., 2017. Ecological stoichiometry beyond redfield: An ionomic perspective on elemental homeostasis. Front. Microbiol. 8, 722.

Ji, Juping, Milne, Russell, Wang, Hao, 2023. Stoichiometry and environmental change drive dynamical complexity and unpredictable switches in an intraguild predation model. J. Math. Biol. 86 (2), 31.

Jiao, Yiying, Zhu, Yongjie, Chen, Mo, Wan, Liang, Zhao, Yijun, Gao, Jian, Liao, Mingjun, Tian, Xiaofang, 2022. The humic acid-like substances released from microcystis aeruginosa contribute to defending against smaller-sized microplastics. Chemosphere 303, 135034.

Khoironi, Adian, Anggoro, Sutrisno, Sudarno, 2019. Evaluation of the interaction among microalgae Spirulina sp, plastics polyethylene terephthalate and polypropylene in freshwater environment. J. Ecol. Eng. 20 (6), 161–173.

Lavrinovičs, Aigars, Murby, Fredrika, Zīverte, Elīna, Mežule, Linda, Juhna, Tālis, 2021. Increasing phosphorus uptake efficiency by phosphorus-starved microalgae for municipal wastewater post-treatment. Microorganisms 9 (8), 1598.

Li, Xiong, Wang, Hao, Kuang, Yang, 2011. Global analysis of a stoichiometric producer–grazer model with holling type functional responses. J. Math. Biol. 63 (5), 901–932.

Lin, Wei, Li, Yu, Xiao, Xiaoying, Fan, Fuqiang, Jiang, Jiakun, Jiang, Ruifen, Shen, Yong, Ouyang, Gangfeng, 2023. The effect of microplastics on the depuration of hydrophobic organic contaminants in Daphnia magna: A quantitative model analysis. Sci. Total Environ. 877, 162813.

Liu, Ge, Jiang, Ruifen, You, Jing, Muir, Derek C.G., Zeng, Eddy Y., 2019. Microplastic impacts on microalgae growth: effects of size and humic acid. Environ. Sci. Technol. 54 (3), 1782–1789.

Loladze, Irakli, Kuang, Yang, Elser, James J., 2000. Stoichiometry in producer-grazer systems: linking energy flow with element cycling. Bull. Math. Biol. 62, 1137–1162.

Lu, Yifeng, Zhang, Yan, Deng, Yongfeng, Jiang, Wei, Zhao, Yanping, Geng, Jinju, Ding, Lili, Ren, Hongqiang, 2016. Uptake and accumulation of polystyrene microplastics in zebrafish (Danio rerio) and toxic effects in liver. Environ. Sci. Technol. 50 (7), 4054–4060.

Lusher, Amy, 2015. Microplastics in the marine environment: distribution, interactions and effects. Mar. Anthropogenic Litter 245–307.

Mao, Yufeng, Ai, Hainan, Chen, Yi, Zhang, Zhenyu, Zeng, Peng, Kang, Li, Li, Wei, Gu, Weikang, He, Qiang, Li, Hong, 2018. Phytoplankton response to polystyrene microplastics: perspective from an entire growth period. Chemosphere 208, 59–68.

Martínez-Jerónimo, Fernando, Villaseñor, Rafael, Rios, Guillermo, Espinosa, Félix, 1994. Effect of food type and concentration on the survival, longevity, and reproduction of Daphnia magna. Hydrobiologia 287, 207–214.

Nolte, Tom M., Hartmann, Nanna B., Kleijn, J. Mieke, Garnæs, Jørgen, Van De Meent, Dik, Hendriks, A. Jan, Baun, Anders, 2017. The toxicity of plastic nanoparticles to green algae as influenced by surface modification, medium hardness and cellular adsorption. Aquat. Toxicol. 183, 11–20.

Pan, Ying, Long, Yaoyue, Hui, Jin, Xiao, Weiyi, Yin, Jiang, Li, Ya, Liu, Dan, Tian, Qingdong, Chen, Liqiang, 2022. Microplastics can affect the trophic cascade strength and stability of plankton ecosystems via behavior-mediated indirect interactions. J. Hazard. Mater. 430, 128415.

Peace, Angela, 2015. Effects of light, nutrients, and food chain length on trophic efficiencies in simple stoichiometric aquatic food chain models. Ecol. Model. 312, 125–135.

Peace, Angela, Poteat, Monica D., Wang, Hao, 2016. Somatic growth dilution of a toxicant in a predator–prey model under stoichiometric constraints. J. Theoret. Biol. 407, 198–211.

Peace, Angela, Wang, Hao, 2019. Compensatory foraging in stoichiometric producer–grazer models. Bull. Math. Biol. 81, 4932–4950.

Peace, Angela, Wang, Hao, Kuang, Yang, 2014. Dynamics of a producer–grazer model incorporating the effects of excess food nutrient content on grazer's growth. Bull. Math. Biol. 76, 2175–2197.

Peace, Angela, Zhao, Yuqin, Loladze, Irakli, Elser, James J., Kuang, Yang, 2013. A stoichiometric producer-grazer model incorporating the effects of excess food-nutrient content on consumer dynamics. Math. Biosci. 244 (2), 107–115.

Peeken, Ilka, Primpke, Sebastian, Beyer, Birte, Gütermann, Julia, Katlein, Christian, Krumpen, Thomas, Bergmann, Melanie, Hehemann, Laura, Gerdts, Gunnar, 2018. Arctic sea ice is an important temporal sink and means of transport for microplastic. Nat. Commun. 9 (1), 1505.

Rana, Md Masud, Dissanayake, Chandani, Juan, Lourdes, Long, Kevin R., Peace, Angela, 2019. Mechanistically derived spatially heterogeneous producer-grazer model subject to stoichiometric constraints. Math. Biosci. Eng. 16 (1), 222–233. http://dx.doi.org/10.3934/mbe.2019012.

Raubenheimer, David, Simpson, Stephen J., 1993. The geometry of compensatory feeding in the locust. Animal Behav. 45 (5), 953–964.

Rodrigues, Joana Patrício, Duarte, Armando C., Santos-Echeandía, Juan, Rocha-Santos, Teresa, 2019. Significance of interactions between microplastics and POPs in the marine environment: a critical overview. TRAC Trends Anal. Chem. 111, 252–260.

Salman, Taylan, Temel, Fulya Aydın, Turan, N. Gamze, Ardali, Y., 2016. Adsorption of lead (II) ions onto diatomite from aqueous solutions: Mechanism, isotherm and kinetic studies. Global NEST J. 18 (1), 1–10.

Sazli, Duygu, Nassouhi, Danial, Ergönül, Mehmet Borga, Atasagun, Sibel, 2023. A comprehensive review on microplastic pollution in aquatic ecosystems and their effects on aquatic biota. Aquat. Sci. Eng. 38 (1), 12–46.

Schatz, Greg S., McCauley, Edward, 2007. Foraging behavior by daphnia in stoichiometric gradients of food quality. Oecologia 153, 1021–1030.

Scherer, Christian, Brennholt, Nicole, Reifferscheid, Georg, Wagner, Martin, 2017. Feeding type and development drive the ingestion of microplastics by freshwater invertebrates. Sci. Rep. 7 (1), 17006.

Simpson, Stephen J., Sibly, Richard M., Lee, Kwang Pum, Behmer, Spencer T., Raubenheimer, David, 2004. Optimal foraging when regulating intake of multiple nutrients. Animal Behav. 68 (6), 1299–1311.

Simčič, Tatjana, Anton, Brancelj, 1997. Electron transport system (ETS) activity and respiration rate in five daphnia species at different temperatures. Hydrobiologia 360, 117–125. http://dx.doi.org/10.1023/A:1003117221455,

Sjollema, Sascha B., Redondo-Hasselerharm, Paula, Leslie, Heather A., Kraak, Michiel H.S., Vethaak, A. Dick, 2016. Do plastic particles affect microalgal photosynthesis and growth? Aquat. Toxicol. 170, 259–261.

Sterner, Robert W., Hessen, Dag O., 1994. Algal nutrient limitation and the nutrition of aquatic herbivores. Ann. Rev. Ecol. System. 25 (1), 1–29.

Thieme, Horst R., 2003. Princeton series in theoretical and computational biology. In: Mathematics in Population Biology. Princeton University Press Princeton, NJ, USA.

Thomas, Diana Maria, Snell, Terry Wayne, Jaffar, Sayed Murtaza, 1996. A control problem in a polluted environment. Math. Biosci. 133 (2), 139–163.

Wang, Hao, Kuang, Yang, Loladze, Irakli, 2008. Dynamics of a mechanistically derived stoichiometric producer-grazer model. J. Biol. Dyn. 2 (3), 286–296.

Wang, Hao, Lu, Zexian, Raghavan, Aditya, 2018. Weak dynamical threshold for the "strict homeostasis" assumption in ecological stoichiometry. Ecol. Model. 384, 233–240.

Wang, Hao, Sterner, Robert W., Elser, James J., 2012. On the "strict homeostasis" assumption in ecological stoichiometry. Ecol. Model. 243, 81–88.

Wang, Mengjing, Wang, Wen-Xiong, 2023. Selective ingestion and response by daphnia magna to environmental challenges of microplastics. J. Hazard. Mater. 131864.

Wang, Qiongjie, Wangjin, Xiaoxue, Zhang, Yong, Wang, Ningxin, Wang, Yulai, Meng, Guanhua, Chen, Yihua, 2020. The toxicity of virgin and UV-aged PVC microplastics on the growth of freshwater algae chlamydomonas reinhardtii. Sci. Total Environ. 749, 141603.

Wu, Di, Wang, Ting, Wang, Jing, Jiang, Lijuan, Yin, Ying, Guo, Hongyan, 2021. Size-dependent toxic effects of polystyrene microplastic exposure on microcystis aeruginosa growth and microcystin production. Sci. Total Environ. 761, 143265.

Xie, Tian, Yang, Xianshan, Li, Xiong, Wang, Hao, 2018. Complete global and bifurcation analysis of a stoichiometric predator-prey model. J. Dynam. Differential Equations 30, 447–472.

Yang, Wenfeng, Gao, Xinxin, Wu, Yixiao, Wan, Liang, Tan, Lichen, Yuan, Shaoman, Ding, Huijun, Zhang, Weihao, 2020. The combined toxicity influence of microplastics and nonylphenol on microalgae Chlorella pyrenoidosa. Ecotoxicol. Environ. Saf. 195, 110484.

Yokota, Kiyoko, Waterfield, Holly, Hastings, Cody, Davidson, Emily, Kwietniewski, Edward, Wells, Britney, 2017. Finding the missing piece of the aquatic plastic pollution puzzle: interaction between primary producers and microplastics. Limnol. Oceanogr. Lett. 2 (4), 91–104.

Zhang, Cai, Chen, Xiaohua, Wang, Jiangtao, Tan, Liju, 2017. Toxic effects of microplastic on marine microalgae Skeletonema costatum: interactions between microplastic and algae. Environ. Pollut. 220, 1282–1288.